

Effects of Helix Dipole Membrane Field Potential Interactions on Hydrophobic Energies
of Transmembrane Proteins

A Thesis submitted
to the Graduate School
Valdosta State University

in partial fulfillment of requirements
for the degree of

MASTER OF SCIENCE

in Biology

in the Department of Biology
of the College of Arts and Sciences

May 2018

Josephine G. Shieh

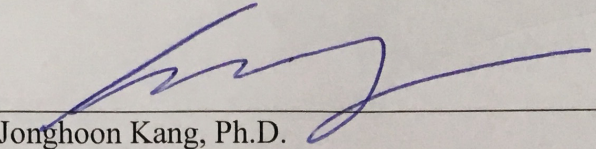
BS, The University of Georgia, 2013

© Copyright 2018 Josephine G. Shieh

All Rights Reserved

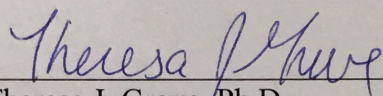
This thesis, "Effects of Helix Dipole Membrane Field Potential Interactions on Hydrophobic Energies of Transmembrane Proteins," by Josephine G. Shieh, is approved by:

**Thesis
Chair**

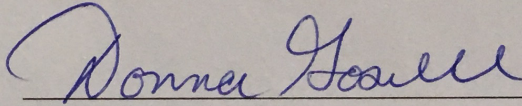


Jonghoon Kang, Ph.D.
Professor of Biology

**Committee
Member**

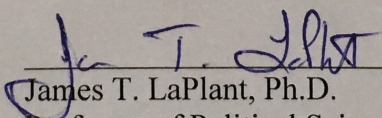


Theresa J. Grove, Ph.D.
Professor of Biology



Donna Gosnell, Ph.D.
Associate Professor of Chemistry

**Dean of the
Graduate School**



James T. LaPlant, Ph.D.
Professor of Political Science

Defense Date

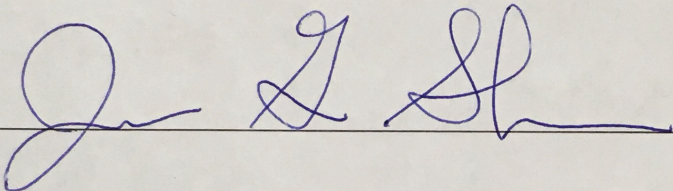
3/30/18

FAIR USE

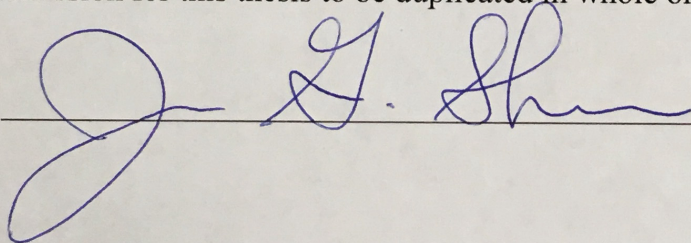
This thesis is protected by the Copyright Laws of the United States (Public Law 94-553, revised in 1976). Consistent with fair use as defined in the Copyright Laws, brief quotations from this material are allowed with proper acknowledgment. Use of the material for financial gain without the author's expressed written permission is not allowed.

DUPLICATION

I authorize the Head of Interlibrary Loan or the Head of Archives at the Odum Library at Valdosta State University to arrange for duplication of this thesis for educational or scholarly purposes when so requested by a library user. The duplication shall be at the user's expense.

Signature 

I refuse permission for this thesis to be duplicated in whole or in part.

Signature 

ABSTRACT

The race to uncover new biological drug targets has led to an emerging field of research on the thermodynamic properties that stabilize transmembrane proteins as well as the role of these stabilizing factors in shaping the evolutionary landscape of drug target populations. When proteins are inserted into the plasma membrane, they fold into three-dimensional secondary protein structures called alpha helices. The electrical interactions within the alpha helix causes the protein to form a macrodipole. As a result of this phenomenon, the energetic stabilities of TM proteins may either be disrupted or enhanced due to the interactions between the surrounding membrane potential and the charged dipole termini of the folded helix. Currently, the relative contributions of compensatory factors to TM protein stability and their population distributions are poorly understood. In this study, two categories of bitopic proteins and the hydrophobic energies of their TM domains were investigated. We hypothesized that Type I TM proteins exhibit lower hydrophobic free energies as a compensatory response to the decreased electrical stabilities of Type I proteins that have incurred an energetic penalty due to the spatial orientations. A Z test showed that Type I proteins exhibit significantly lower hydrophobic free energies than Type II proteins ($p = 0.0003$, $\alpha = 0.05$). A Z test of Shannon entropies of both protein types revealed that Type 1 proteins exhibit significantly lower Shannon entropies than those of Type 2 ($p = 0.000$, $\alpha = 0.05$). Linear regression analysis showed a weak correlation between Type I Shannon entropies and Type I hydrophobic energies ($R^2 = 0.221$) and Type II Shannon entropies and Type II hydrophobic energies ($R^2 = 0.232$), suggesting that Shannon entropies are not a direct function of hydrophobic free energies and may arise from synergistic interactions among various energetic contributors.

TABLE OF CONTENTS

I. INTRODUCTION.....	1
II. REVIEW OF LITERATURE	6
Type I and Type II Proteins	6
The Alpha Helix Dipole	7
Electrical Properties of Cellular Membranes	11
Determinants of Protein Stability	13
Hydrophobicity Scales	15
Functional Significance of Transmembrane Domains	16
III. MATERIALS AND METHODS	18
Data Collection.....	18
Retrieval of Type I and Type II Protein Accession Numbers	18
Retrieval of Transmembrane Domain Residue Sequences	18
Retrieval of Grand Average of Hydropathicity Values	19
Retrieval of Kyte and Doolittle Hydropathy Indices	19
Retrieval and Determination of Protein Functional Class	20
Mathematical Computation	20
Computation of Gibb's Free Energy	20
Computation of Hydrophobic Energies	20
Computation of Shannon Entropies	21
Statistical Analysis.....	22
Monte Carlo Simulation of Normal Distribution of Hydrophobic Energies	22
Shapiro Wilk Test of Gaussian Normality of Hydrophobic Energies	22

Levene's Test of Equality of Variances of Hydrophobic Energies	23
Mann-Whitney U Test of Hydrophobic Energies	23
Z Test of Hydrophobic Energies	24
Monte Carlo Simulation of Normal Distribution of Shannon Entropies	24
Shapiro Wilk Test of Gaussian Normality of Shannon Entropies	25
Levene's Test of Equality of Variances of Shannon Entropies	25
Mann-Whitney U Test of Shannon Entropies	25
Z Test of Shannon Entropies	26
Linear Regression of Hydrophobic Energies and Shannon Entropies	27
IV. RESULTS.....	28
Gibb's Free Energy Difference	28
Frequency Distributions of Hydrophobic Energies	28
Mann-Whitney U Test of Hydrophobic Energies	30
Z Test of Hydrophobic Energies	32
Frequency Distributions of Shannon Entropies	32
Mann-Whitney U Test of Shannon Entropies	34
Z Test of Shannon Entropies	36
Shannon Entropy as a Function of Hydrophobic Energy	36
Functional Classification	39
V. DISCUSSION.....	40
Hydrophobic Energy Compensation	40
Z Test of Transmembrane Domain Hydrophobic Energies	40
Z Test of Transmembrane Domain Shannon Entropies	41

Linear Regression Analysis of Shannon Entropy as a Function of Hydrophobic	
Energy	42
Functional Classification	43
Summary.....	43
REFERENCES.....	45
APPENDIX A: Kyte and Doolittle Amino Acid Hydrophobicity Indices	49
APPENDIX B: Type I Hydrophobic Energies and Shannon Entropies	51
APPENDIX C: Type II Hydrophobic Energies and Shannon Entropies	77

LIST OF FIGURES

Figure 1: Schematic of protein macrodipole in membrane potential field11

Figure 2: Frequency distribution of Type I TM protein hydrophobic energies29

Figure 3: Frequency distribution of Type II TM protein hydrophobic energies29

Figure 4: Frequency distribution of Type I TM protein Shannon entropies33

Figure 5: Frequency distribution of Type II TM protein Shannon entropies33

Figure 6: Linear regression plot of Type I Shannon entropies as a function of Type I hydrophobic energies37

Figure 7: Linear regression plot of Type II Shannon entropies as a function of Type II hydrophobic energies38

Figure 8: Classification of Protein Functions39

LIST OF TABLES

Table 1: Mean ranks of Type I and Type II TM protein hydrophobic energies31

Table 2: Asymptotic two-tailed p value of Mann-Whitney U test of hydrophobic energies.....31

Table 3: Left-tailed p value of Mann-Whitney U test of hydrophobic energies31

Table 4: Mean ranks of Type I and Type II protein Shannon entropies35

Table 5: Asymptotic two-tailed p value of Mann-Whitney U test of Shannon entropies.. 35

Table 6: Left-tailed p value of Mann-Whitney U test of Shannon entropies35

Table 7: ANOVA table of linear regression analysis of Type I Shannon entropies plotted as a function of Type I hydrophobic energies.....37

Table 8: ANOVA table of linear regression analysis of Type II Shannon entropies plotted as a function of Type II hydrophobic energies.....38

ACKNOWLEDGEMENTS

I would like to express my gratitude to my major advisor, Dr. Jonghoon Kang, for his instruction, patience, and unwavering enthusiasm and faith in this project, all the miles he walked from his office to my office, and his mentorship in helping me to see this project through to its completion.

I would also like to thank Dr. Theresa Grove for her invaluable wisdom and levelheadedness and Dr. Donna Gosnell for her constant support and advice.

I cannot express enough thanks to Dr. Teresa Doscher for her care and mentorship in my laboratory teaching duties.

I am also grateful to Dr. Emily Cantonwine, Dr. Mark Blackmore, Dr. Timothy Henkel, and Dr. Jennifer Turco for their instructional guidance in my academic courses during my time in this program.

Special thanks to Mrs. Regina Ogden, Dr. Jim Loughry, and Dr. Robert Gannon for their support and advice outside of academics and research.

And last, but certainly not least, I would like extend my utmost appreciation to all of my fellow graduate students for their mutual support and care during our time together in this program.

DEDICATION

To God who has shepherded me all my life and my mom.

Chapter I

INTRODUCTION

Natural selection is the primary mechanism that is hypothesized to govern evolutionary processes, and evolutionary outcomes are theorized to be constrained by the criteria of achieving increased fitness. Yet, differences in the persistence of populations, and their resulting sizes can also be explained by the necessity to conform to the thermodynamic principles that govern energy infrastructures within biological systems. The direction of evolution is driven by the minimization of the total Gibb's free energy in a system. This minimal energy criterion is contingent upon the second law of thermodynamics, which favors entropy maximization (Jia, Liggins, & Chow, 2014). Disparities in thermodynamic fitness, which may arise from interactions among various factors including environment and phenotype, can prompt adaptive responses from other components within a system in order to maintain overall thermodynamic stability.

If the evolutionary constraints exerted upon the system persist and are quite strong, compensatory responses may also be conserved over time within a population. One example of a molecular system that is not exempt from the principle of minimal energy is membrane proteins. The unfavorable interactions between the termini of membrane protein dipoles and their electrically charged environments may be recognized by protein selection and insertion machinery (Agnati et al., 2005). As a result, proteins with greater stabilizing characteristics, such as high hydrophobic energies, may be selected for insertion within the hydrocarbon cores of cellular membranes in order to

compensate for their otherwise high instabilities. However, few studies have investigated this hypothesis.

Understanding the thermodynamics underlying membrane protein stability is desirable for many reasons. Membrane proteins account for roughly one-third of all sequenced proteins and are one of the most important features of cellular systems (Hubert et al., 2010). These proteins play diverse roles in the normal functioning of cells and are involved in various functions, including cell-cell adhesion, molecular transport, ion regulation, signal transduction, enzyme catalysis, and immune pathways. Since membrane proteins are key components of cellular defense pathways, a fundamental understanding of the thermodynamic mechanisms underlying their stability and functioning is essential to drug development initiatives. In fact, bitopic membrane proteins account for more than 60% of all known drug targets encoded by the human genome (Yin & Flynn, 2016).

Currently, most exogenous agonists are designed to inhibit, activate, or modify cell signaling pathways by selectively binding to protein moieties acting as cell-surface receptors and subsequently triggering or suppressing associated effector and second messenger cascades. Therapeutic ligands are designed to adhere exclusively to exposed peptide regions that are easily accessible on the surface of the bilayer. In fact, G-protein coupled receptors account for one-third of drug targets (Dror et al., 2011). Yet, therapeutic agents are seldom designed to directly target transmembrane domains embedded deep in the interior of the hydrophobic bilayer.

The tendency to develop therapeutics that target exposed protein segments instead of those that target protein segments embedded within the bilayer's hydrophobic core can

be attributed to several factors. First, the process of accessing the hydrophobic core of the plasma membrane is experimentally complex and often difficult to achieve. Steroids and small nonpolar molecules characterized by high permeability are able to passively diffuse across the transmembrane region of the bilayer, but the passage of the majority of large polar molecules involves transport-mediated or endocytic pathways. Although not altogether impossible, the translocation of proteins and small peptides across membranes is rare (Yang & Hinner, 2016). Another perceived barrier to the viability of transmembrane drug targets is that drug targets require high specificity, but it is still unknown which specific regions of the transmembrane region could serve as potential drug targets.

Second, the erroneous concept that transmembrane domains serve no other purpose than to anchor the protein within the bilayer is, unfortunately, quite prevalent. The idea that transmembrane domains do not engage in meaningful interactions that are subject to drug targeting still informs much of the development of biopharmaceuticals. This notion is gradually changing as experimental evidence is accumulating that shows the functional importance of transmembrane domains. Nevertheless, the properties of transmembrane domains involved in disease pathways has remained relatively underexplored compared to the attention that has been paid to their extracellular counterparts. Experiments examining the extent to which the hydrophobicities of transmembrane helices serve as an energetic hindrance to retrotranslocation by endoplasmic reticulum associated degradation (ERAD) pathways during protein misfolding have been performed, but information regarding the general mechanism and details underlying transmembrane domain removal from the bilayer preceding

degradation is scarce (Guerriero et al., 2017). Exacerbating the inattention to transmembrane drug targets is the dearth of available information on membrane protein three-dimensional structure (Opella & Marassi, 2004). In fact, only 2% of structures in the Protein Database Bank belong to membrane proteins (Zhou, Zheng, & Zhou, 2004). Ultimately, the reality remains that the number of available extracellular drug targets encoded by the human genome is finite. When pharmacotherapy has exhausted the study of extracellular drug targets, the pressure and the demand for the study and identification of novel drug targets and their biophysical properties will inevitably increase.

In spite of the biases underlying drug research, the advancement of existing and novel biotechnological methods is helping to redefine the notion of what makes molecular moieties targetable. Advances in X-ray crystallography, cryoelectron microscopy, and nuclear magnetic resonance spectroscopy are contributing to the growing database of available membrane protein structures and protein-protein interactions and could greatly help to inform structure-based rational design (Punta et al., 2007). The refinement of ToxR, an experimental method that probes interactions among transmembrane domains, is another promising advancement in the quest for information on transmembrane domain interactions. In addition, the discovery of highly specific and localized protein-protein interaction hot spots has encouraged the development of drugs that exclusively target these critical areas. The novel synthesis of molecular mimics that influence transmembrane domain-domain interactions also represents an alternative method of drug delivery. For example, small molecules have been identified that target Toll-like Receptor one and two, a key player in Parkinson's disease.

In light of the evolving definition of what constitutes a good drug target and the rapid pace of biotechnological development, research on the fundamental properties of transmembrane domains is essential. It is incumbent upon the scientific community to ensure that the availability of information on transmembrane domains and the interactions among them progresses at a rate equal to that of biotechnological advances. In anticipation of the emerging need for more information on the physicochemical properties of transmembrane domains, we performed a comparative study that characterizes the stabilizing properties of transmembrane proteins, namely the hydrophobic free energies of their hydrophobic domains. In this study, we identified statistical differences between the hydrophobic free energies and Shannon entropies of two groups of bitopic proteins. A weak correlation between hydrophobic free energies and Shannon entropies was determined, and further research is needed in order to elucidate the precise mechanisms underlying the correlation between these two parameters.

Chapter II

REVIEW OF LITERATURE

Type I and Type II Proteins

Membrane proteins are proteins that are embedded in the plasma membrane, a lipid bilayer that serves as a selectively permeable barrier between the interior cellular environment and the surrounding extracellular space. Two classes of membrane proteins are peripheral and integral membrane proteins. Peripheral membrane proteins are water-soluble proteins that are attached to the exterior surface of the plasma membrane, while integral membrane proteins are proteins that have one or more regions embedded in the hydrophobic core of the lipid bilayer. Integral membrane proteins that have backbones that transverse the entire length of the phospholipid bilayer are called transmembrane proteins (Cooper, 2000). Transmembrane proteins consist of bitopic and polytopic proteins. Bitopic proteins cross the bilayer only once. Examples of bitopic proteins include Type I, Type II, and Type III proteins. Polytopic proteins, such as Type IV proteins, cross the bilayer more than once (Zviling, Kochva, & Arkin, 2007).

Type I and Type II TM proteins are polymers composed of individual monomeric amino acid units held together by peptide bonds. They typically exist as a distinct type of secondary structure protein called an alpha helix and assume the three-dimensional shape of a coil or a screw that is held together by hydrogen bonds (Albers, 1999). In terms of chirality, most alpha helical proteins are right handed (Cole & Bystroff, 2009). Type I membrane proteins are characterized by a signal peptide sequence that is approximately

15 hydrophobic amino acid residues in length and is subsequently cleaved from the rest of the peptide. The signal that cues the protein to remain embedded in the membrane instead of being completely threaded through is called a stop-transfer sequence, which is composed of approximately 20 hydrophobic amino acid residues. The signal peptide sequence and the stop transfer sequence result in the translocation of the peptide's N-terminus across the membrane.

In contrast to Type I membrane proteins, Type II membrane proteins contain a signal-anchor sequence that is approximately 25 hydrophobic amino acid residues in length and are much longer than Type I signal sequences. Type II signal-anchor sequences are characterized by the absence of a signal peptidase cleavage site and are therefore not cleaved after translocation occurs. Type II signal-anchor sequences result in the translocation of the peptide's C-terminus across the membrane. Type I proteins have their positively-charged amino group oriented towards to the extracellular space while their negatively-charged carboxyl groups are oriented towards the cytoplasmic interface. Type II proteins have their negatively-charged carboxyl groups oriented towards the extracellular space, while their positively-charged amino groups are oriented towards the cytoplasmic compartment. Thus, Type I and Type II proteins are opposites of each other in terms of their orientations within the membrane (Goder & Spiess, 2001).

The Alpha Helix Dipole

Peptide bonds within Type I and Type II proteins produce individual dipoles. Each protein has a net dipole moment with two polarized termini that is calculated from the sum of the individual dipole moments of peptide bonds (Moran, Horton, Scrimgeour, & Perry, 2011). A dipole moment is a vector value that quantifies and describes the

electrical polarity of a molecule. A dipole moment is formed when a molecule contains atomic regions that possess a partial positive or partial negative charge and are spatially arranged in such a way so that they do not cancel one another out. Electronegativity is a measure of an atom's affinity for electrons in a bond, and unequal charge distributions in a molecule arise due to differences in the electronegativities of the individual atoms comprising that molecule. Dipole moments can occur in both diatomic and polyatomic molecules. In a diatomic molecule containing two covalently bonded atoms possessing unequal electronegativities, the more electronegative atom will attract electrons (negatively charged particles) to itself and acquire a partial negative charge, while the less electronegative atom will acquire a partial positive charge. In general, a dipole moment can be calculated using the following equation: $\mu = q \times r$, where μ is the size of the dipole moment, q is the charge, and r is the distance of separation between the two charges. The unit symbol of a dipole moment is D, which stands for units of Debye. In artistic renderings, the dipole moment can be drawn as an arrow with a cross tail. While many chemistry textbooks render the tip of the arrow to denote the negative pole and the crossed tail to denote the positive pole, physics conventions use IUPAC nomenclature and represent the tip of the arrow as the positive pole and the crossed tail as the negative pole (Parkanyi, 1998).

Proteins are composed of amino acids joined by a peptide bond, a type of covalent bond. Each amino acid is composed of an alpha carbon, a hydrogen, a unique side chain residue, an amino group (-NH₂), and a carboxyl group (-COOH). A dehydration synthesis reaction produces a peptide bond between two individual amino acids and releases a water molecule. At physiological pH, amino acids exist as zwitterions, and

their structures are represented differently from their representations in theoretical reactions, but the process is relatively the same. In the theoretical condensation reaction, the lone pair of electrons on the nitrogen of the amino group will perform a nucleophilic attack on the carbon of the carboxyl group. As a result, the pre-existing lone pair of electrons on the nitrogen will form a new bond between the amide nitrogen and the carbonyl carbon. This results in carbon having 10 valence electrons, which violates the octet rule, which leads to the hydroxyl (-OH) that comprises the carboxyl group on the first amino acid being protonated when it binds to a hydrogen in the amino group of the second amino acid. The -OH will remove the two electrons it originally shared with carbon and use them to form a bond to a hydrogen of the second amino acid. The combination of -OH and -H forms a water molecule. The lone pair of valence electrons that is left by the hydrogen may either: continue to exist as a lone pair on the nitrogen or form a second bond between the nitrogen and the carbon, which creates partial double bond character to the N-C of the peptide bond; this delocalization of electrons is called resonance. Apart from the structural stability that it confers to a peptide bond, resonance paradoxically also confers stereochemical variation. Since the amide nitrogen's electrons are delocalized, the dipeptide segment is a stereoisomer that can assume one of two isomeric forms (cis- or trans-) in three-dimensional space. The cis- isomer is when the functional groups are on the same side, while the trans- isomer is when the functional groups are on opposite sides. At physiological conditions, the majority of dipeptide segments exist in the trans- form. When dipeptide segments exist in a trans orientation, the arrangement of atoms permits a dipole to form.

A peptide bond's dipole moment is due to differences in electronegativity between two pairs of atoms. The first pair of atoms is the oxygen and the carbon in the amino acid's carbonyl group. Since oxygen's electronegativity is greater than that of carbon, the oxygen will assume a partial negative charge (-0.42) and the carbon will assume a partial positive charge (+0.42). The second pair of atoms is the nitrogen and the hydrogen in the amino acid's amino group. Since nitrogen's electronegativity is greater than that of hydrogen, the nitrogen will assume a partial negative charge (-0.20) and the hydrogen will assume a partial positive charge (+0.20). Both dipole moments formed by each pair of atoms exist parallel to the helix axis. In addition, the alpha helix contains three types of torsional angles: ω , ϕ , and ψ . Ramachandran plots are plots of the ϕ (phi) angles against the ψ (psi) angles; the presence of clusters indicates that a helix possesses a regular repeating structure. Since Ramachandran plots indicate that the ϕ and ψ angles of each amino acid in a helix are very similar (-57° and -47° , respectively), the alpha helix exhibits structural regularity. Structural regularity is vital to preventing the disruption of a helix's net dipole moment. Since the alpha helix is composed of 3.6 residues per turn and contains multiple repeating turns depending on its length, it contains multiple peptide bonds. The individual dipole moments of each peptide bond will result in a net dipole moment called a macrodipole with charged terminal ends, where the amino terminus is positive and carboxyl terminus is negative. Since the dipole moment of a single peptide bond is 3.6 D, the macrodipole of an alpha helix can be calculated as the number of amino acid residues times 3.6 D.

Electrical Properties of Cellular Membranes

Cellular systems are characterized by the presence of an electrical gradient at the membrane boundary. These electrical gradients confer a positive charge along the membrane-extracellular space (ECS) interface and a negative charge along the membrane-cytoplasm interface. This electrical gradient is called membrane potential, which is analogous to an electromagnetic field. When magnetic dipoles are placed in electric fields, their energetic stability may be high or low. Similarly, when TM proteins are placed within membranes having membrane potential, their energetic stabilities may be disrupted or enhanced due to the interactions between the voltage gradient and the charged dipole termini of native proteins (Figure 1).

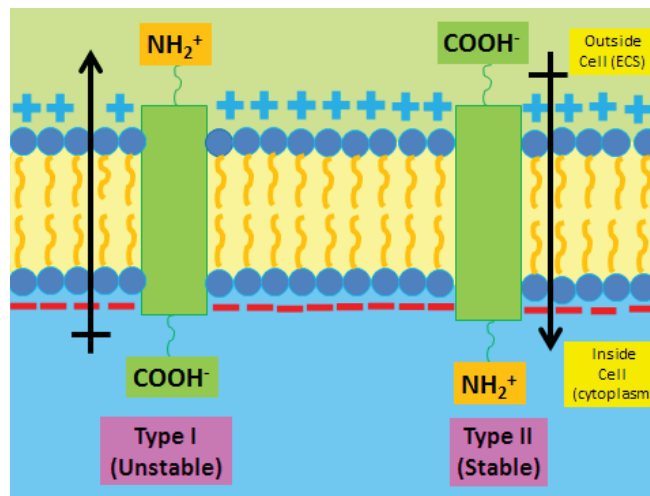


Figure 1. Schematic of protein macrodipole in membrane field potential

The difference in the orientations of Type I and Type II membranes suggests that there is also a difference in electrical energy between these two transmembrane proteins. Type I proteins may exhibit greater thermodynamic instability due to the interactions between their negatively-charged carboxyl groups and the negatively charged membrane-

cytoplasm interface. Type II proteins may exhibit less thermodynamic instability due to the interactions between their positively-charged amino groups and the positively-charged membrane-ECS interface. This observation is based on Coulomb's law, which simply states that oppositely charged particles tend to attract, while similarly charged particles tend to repel. These principles are illustrated by potential energy curves, which demonstrate that as the distance between like-charges decreases (as they move closer together), their repulsive potential energy increases; however, as the distance between opposite charges decreases (as they move closer), their repulsive potential energy decreases.

It is possible to measure the strength of attractive and repulsive forces using Coulomb's law, which measures the strength of the force/energy between a pair of charges in joules (J). Attractive forces are indicated by negative signs (gained by the product of two opposite charges), while repulsive forces are indicated by positive signs (a result of the product of two similar charges). In the following formula, k is a constant of $2.31 \times 10^{-19} \text{ J} \cdot \text{nm}$, Q_1 and Q_2 represent the quantities of the charges on each respective particle, and r is the distance between the two atoms:

$$F = \frac{kQ_1Q_2}{r^2}$$

The degree of a force (whether attractive or repulsive) between two atoms is the product of the two charges on both atoms divided by measure of the distance between them multiplied by the constant, k . Thus, as a result of this biophysical dynamic, Type I proteins may exhibit greater electrochemical instability. The former situation results in greater thermodynamic stability, while the latter situation results in lower thermodynamic instability. Since the configurations of Type I proteins represent the latter situation, they

are, in effect, at a greater energy disadvantage due to their orientation within cellular membranes.

Determinants of Protein Stability

The properties of lipid bilayers that surround membrane proteins are one of the determinants of membrane protein stability are the properties of the lipid bilayers that surround membrane proteins (Van Klompenburg, Nilsson, von Heijne, & de Kruijff, 1997). Unlike the substances that solvate globular proteins, the lipid medium is far from isotropic. The plasma membrane is composed of a variety of different lipids, and certain types of lipids are more abundant in certain areas of the bilayer. For example, the extracellular outer leaflet usually contains high amounts of sphingolipids, glycolipids, and phosphatidylcholine, while the cytoplasmic inner leaflet usually contains phosphatidylserine, phosphatidylethanolamine, and phosphatidylinositol. Some lipids, such as cholesterol, are evenly distributed throughout both layers and may cause fluctuations in the permeability of the membrane. Such disruptions to membrane permeability may influence protein stability. The disparities in regional lipid composition along a membrane may primarily be attributed to the presence of lipid rafts. Lipid rafts are lipid-dense areas along the plasma membrane that contain localized and unique concentrations of sphingolipids, cholesterol, and proteins (Pike, 2003). The ability of components to be recruited to or disassociate from lipid rafts and the ability of rafts to move laterally and combine with other rafts (in a process called raft clustering) make the lipid composition of these areas highly dynamic.

The high variety of lipids that comprise membranes may be due to the corresponding diversity of proteins that they solvate and the interactions that occur

between them amidst fluctuations in temperature, osmolarity, pH, and supramolecular lipid polymorphisms (Simons & Sampaio, 2011). A membrane protein's ability to function depends on the presence of particular lipids having specific head groups or hydrocarbon tails that may serve to optimize its functionality (Deol, Bond, Domene, & Sansom, 2004). Furthermore, the chemical composition of a lipid membrane encasing a particular organelle may be very different from those of other organelles. Studies have also found that the electrostatic properties of membrane voltage gradients are dependent upon the compositions of the lipids that generate them (Gurtovenko & Vattulainen, 2008). Similarly, the lengths of lipids that comprise the membrane help determine the thickness of the phospholipid bilayer (Lee, 2004). On average, the polar headgroups of lipids are 15 Å, and their hydrophobic regions are 30Å (Haltia & Freire, 1995). Yet, differences in lipid composition in certain regions of the bilayer may result in variations in membrane thickness along the circumference of the cell (Nagle & Tristram-Nagle, 2000). It has been shown that fluctuations in temperature may affect lipid thickness as well (Simon, Advani, & McIntosh, 1995).

Apart from influencing the electrostatic gradients across membranes, variations in the thickness of the bilayer are important, since it may also affect the angle at which a membrane protein is tilted perpendicular to the membrane plane (Kim & Im, 2010). Multiple studies have shown that when bilayer thickness is shortened, protein tilt angle — the angle formed by the protein and the axis perpendicular to the membrane plane — increases (Holt et al., 2009). The biological phenomenon in which a discrepancy exists between the length of the transmembrane helix and membrane thickness is called hydrophobic mismatch (de Jesus & Allen, 2013). Changes in tilt angle in response to the

shortening of the bilayer occur in order to optimize the retention of the peptide's transmembrane helix and hydrophobic residues within the hydrophobic core (Park & Opella, 2005). In addition, it has also been observed that helices may bend and stretch in response to hydrophobic mismatch (de Jesus & Allen, 2013).

Hydrophobicity Scales

Hydrophobicity is a quantitative measure used to determine how anchored a protein is within the membrane. Hydrophobicities are represented as GRAVY values and are computed as the average of the hydrophobicities of each amino acid within a polypeptide sequence. A hydrophobicity scale assigns a hydrophathy value to each of the 20 amino acids. Several hydrophobicity scales are available, and each scale is constructed using different methods. The Kyte and Doolittle (KD) hydrophobicity scale is one of the most widely used hydrophathy scales in the field of biophysics (Appendix A). In the Kyte and Doolittle scale, the majority of the hydrophathy values for each individual amino acid were determined by averaging two or three normalized values (Kyte & Doolittle, 1982). The first value is the transfer free energies from water to vapor ($\Delta G^{\circ}_{\text{water} \rightarrow \text{vapor}}$) in kcal/mol. This value was used in lieu of the transfer free energies from water to ethanol and ethanol to vapor, due to the non-neutral properties of ethanol. The water-vapor transfer partition coefficients were based on model substances equivalent to each amino acid residue and represent a compilation of data collected by scientists including Hine and Mookerjee (1975) and Wolfenden, Cullis, & Southgate (1979). Chothia (1976) used twelve globular native structures and their coordinates to record the number of times a particular amino acid residue was found to be 95% buried within the interior of the protein. This value was then divided by the total number of that

occurring residue. Thus, the second value is the fraction of residues that are 95% buried, and the third value is the fraction of residues that are 100% buried.

Functional Significance of Transmembrane Domains

Apart from securing membrane proteins in the bilayer, transmembrane domains play many important roles in the biological and biochemical functions of proteins involved in disease pathways. For example, mutations in the third transmembrane domain of the melanocortin-4 receptor (MC4R) – a G protein-coupled receptor, that has been identified as a cause of obesity – significantly affect ligand binding, signaling, and second messenger production (Mo, Yang, & Tao, 2012). Similarly, experiments have shown that transmembrane domains of a viral membrane protein called LMP-1 are primarily involved in signaling activity of the Epstein-Barr virus (Kaykas, Worringer, & Sugden, 2002). It has been found that mutations in transmembrane domains of the diphtheria fusion protein toxin DAB3890-IL-2 can alter cytotoxicity (VanderSpek, Mindell, Finkelstein, & Murphy, 1993). Mutations in transmembrane domains of penicillin binding proteins in *S. pneumoniae* have given rise to morphological modifications in cells, which shows the importance of transmembrane domains in peptidoglycan construction (Berg et al., 2014). Furthermore, the transmembrane domains of a kidney-lung sodium channel complex are responsible for indicating degradation by endoplasmic reticulum chaperones (Buck et al., 2017). In addition, transmembrane domains have also been found to facilitate the dimerization of toll-like receptor (TLR) proteins (Godfroy, Roostan, Moroz, Korendocych, & Yin, 2012). Other scientists have found that survival proteins mediate apoptosis inducing proteins, such as Bax, through transmembrane domain mediated associations (Andreau-Fernandez, 2017).

Transmembrane domains are also known to influence the energetic interactions within cells. The transmembrane domain of the Influenza A viral M2 proton channel is responsible for proton translocation (Hu et al., 2007). Transmembrane domains also have biophysical implications on the characteristics of membrane proteins. For example, the macrodipole of transmembrane proteins significantly contributes to the ability of proteins to participate in helix-bundle aggregation and their transport capabilities. Helices that comprise a bundle are often positioned antiparallel to one another due to the increased stabilization that is conferred. In turn, aggregation and orientation can greatly influence the variable functional capabilities of the membrane proteins and those of the aggregates that they form (Brady, Siegel, Albers, & Price, 2012). Hence, transmembrane domains are involved in lateral associations that may result in oligomerization and protein-protein interactions (PPIs).

Chapter III

MATERIALS AND METHODS

Data Collection

Retrieval of Type I and Type II Protein Accession Numbers

Type I and Type II membrane proteins and their accession numbers were retrieved from UniProtKB (<http://www.uniprot.org>). Lists for all Type I and Type II proteins were located by setting the filter function to display proteins by “subcellular location” and inputting “single-pass” in the search bar on the database’s home page. Proteins were sorted by type and stored in Excel spreadsheets. Only proteins that were Swiss-Prot manually annotated and reviewed (via experimental research or computerized prediction models) were selected in order to maintain quality assurance. Proteins found in organisms other than *Homo sapiens* were excluded from this study. Only proteins residing in the plasma membrane were retained.

Retrieval of Transmembrane Domain Residue Sequences

Amino acid sequences comprising the transmembrane regions of all Type I and Type II alpha helical proteins were individually retrieved from each of the protein profiles contained in UniProtKB. Retrieval was accomplished by accessing a particular protein’s profile and selecting the “Subcellular Location” tab on the leftmost menu bar shown on the subsequent interface. The residue sequence was obtained by locating the “Position(s)” column and selecting the range of position numbers displayed adjacent to the “Transmembrane” row in the “Feature Key Table” that is included in the “Topology”

subsection of the protein's profile. All residue sequences were transferred to Excel spreadsheets and stored alongside their corresponding accession numbers.

Retrieval of Grand Average of Hydropathicity Values

Manually computed Grand Average of Hydropathicity (GRAVY) values were validated externally using the integrative ProtParam software tool from the SIB ExPASy (Expert Protein Analysis System) Bioinformatics Resource Portal. This is a supplementary portal that can be accessed from within the UniProtKB database. Within any given protein profile, the "Sequence" tab was selected from the left menu bar and the "ProtParam" option was selected from the dropdown menu bar. The range for a sequence fragment corresponding to "FT TRANSMEM" was selected. Only peptide sequence fragments with endpoints designated "TRANSMEM" were selected for physicochemical properties analysis. The GRAVY value was obtained by locating the computed parameter on the protein analysis interface. ExPASy ProtParam GRAVY values were matched against computed values (based on the same Kyte-Doolittle hydropathy scale) in order to identify errors and inconsistencies in computed values.

Retrieval of Kyte and Doolittle Hydropathy Indices

The Kyte and Doolittle hydropathy indices for all amino acids were obtained by accessing the ExPASy portal's ProtScale tool (<http://www.expasy.org>) and selecting the "Hphob. / Kyte & Doolittle amino acid scale" from the list of available scales. Each amino acid's hydropathy index was imported into Excel. Hydropathy values were validated by directly accessing the original article.

Retrieval and Determination of Protein Functional Class

Functional classes of all proteins were determined by accessing a particular protein's profile and selecting the "Function" tab on the leftmost menu bar shown on the interface of each individual UniprotKb protein profile. All known molecular and biological functions of each protein were retrieved from the "Function" subsection. Enzymatic functions and pathways were retrieved from Reactome, a peer-reviewed external database that can be accessed through UniprotKb (<http://www.reactome.org>). Proteins were classified into one or more of the following functional categories: Enzyme, Receptor, Both Enzyme and Receptor, Immune, Both Immune and Receptor, Transporter, and Other. The function(s) of proteins belonging to the category "Other" were recorded in a separate column.

Mathematical Computation

Computation of Gibb's Free Energy

The electrical free energies (ΔG°) of the dipoles of Type I and Type II alpha helices in the charged membrane field were calculated using the electrical free energy equation: $\Delta G = \mu E$ where μ is the dipole moment charge (1 electron) multiplied by the electron charge (1.6×10^{-19} C) multiplied by the length of the helix (L_h). E is the membrane potential (V_m) divided by the thickness of the membrane (L_m). Here, we make the following assumptions: 1) The length of each helix approximates the thickness of the portion of the membrane it is embedded in, 2) membrane potential is 100 mV.

Computation of Hydrophobic Energies

Following residue sequence retrieval, the hydrophobicity values of all Type I and Type II proteins were manually calculated using UniprotKb. Sequences were

manipulated in Excel and treated as text strings. Alphabet characters comprising each text string sequence were horizontally divided into individual cells. The “text to columns” feature was used to set field widths and create column breaks so that a single letter representing a single amino acid was assigned to a solitary cell. Subsequently, individual hydrophathy indices for all 20 amino acids based on the Kyte-Doolittle scale (Appendix A) were imported from ExPASy and assigned to their corresponding amino acid symbol in Excel. All amino acids were replaced with their corresponding scale values using the “substitution” feature. GRAVY values for all proteins were calculated as the average (the sum of the hydrophathy values of all constituent amino acids divided by the number of residues in the sequence) of each alpha helix’s amino acid constituents. GRAVY values were then multiplied by the number of amino acid residues in each protein’s transmembrane domain. GRAVY values were converted from units of kcal/mol to units of kJ/mol.

Computation of Shannon Entropies

Information entropies of both groups of transmembrane proteins were determined and compared. The following formula was used to compute Shannon entropies (SE): $SE = -\sum P \log_2 P$, where P is the probability of a given amino acid within a given protein’s residue sequence. Amino acid text sequences were converted to columns and column breaks were inserted. The “substitution” feature was used to replace each amino acid letter symbol with the number 1, and the “=SUM” formula was used to compute the number of times an amino acid appeared within a given sequence. Once the frequency of appearance was calculated, the 1s were replaced with the amino acid letter symbol once more. As a precautionary measure, the number zero was used to replace all ones in order

to ensure that if ones were not replaced with their amino acid letter symbol for any reason, that the retained ones would not affect the subsequent frequencies of the next amino acid being summed. This procedure was performed for all 20 amino acids for all proteins. Once the frequencies of all amino acids were calculated, the lengths of each sequence was calculated using the “=LEN(first cell, last cell)” formula. The probability value of each amino acid was computed by dividing the amino acid frequencies by the length of the entire protein. In order to achieve this, the conditional formula function “=IF(probability = 0, 0, probability *(LOG(probability, 2)))” was used. Following this step, the “pLog₂P” amino acid values for each row were summed to yield the Shannon entropies of each transmembrane protein.

Statistical Analysis

Monte Carlo Simulation of Normal Distribution of Hydrophobic Energies

A random number generator in Excel was used to generate 10,000 random transmembrane amino acid residue sequences. Hydrophobic energies for each sequence was calculated, and a frequency distribution of all sequence hydrophobic energies was created in order to ensure that the hydrophobic energies of the random sequences were normally distributed.

Shapiro Wilk Test of Gaussian Normality of Hydrophobic Energies

In order to determine if the assumption of normality required by the Student's t test were met by the data, Statistical Package for the Social Sciences (SPSS) software was used to perform a Shapiro Wilk test. Both Type I and Type II proteins along with their respective hydrophobic energies were transferred to a new data sheet in SPSS. The “Analyze” tab was selected from the top menu bar, and the “Explore” function was

selected. Type was moved to the “Factor List” space and Hydrophobic Energy was moved to the “Dependent List.” The “Statistics” tab was opened and used to set the “Confidence Interval for the Mean” to 95%. Only the “Descriptives” box was checked. The “Plots” tab was opened and “Normality plots with tests” was checked. No changes were made to the “Options” criteria. As a supplement to the Shapiro Wilk test, histograms showing the frequency distributions of both Type I and Type II protein hydrophobic energies were created in order to provide a secondary visual measure with which to assess the data. To create the histograms, Minitab software was used. The data was transferred into a new spreadsheet, and the “Graphs” tab was used to generate the histograms.

Levene’s Test of Equality of Variances of Hydrophobic Energies

In order to determine if the assumption of equal variances required by the Student’s T test were met by the data, SPSS was also used to perform a Levene’s Test for homogeneity of variances. A Levene’s test for homogeneity of variances was conducted using a “One-Way ANOVA” where default settings for “Contrasts” and Post Hoc Criteria” were used.

Mann-Whitney U Test of Hydrophobic Energies

Following the validation of the assumptions required by the parametric Student’s T test, SPSS was used to perform a non-parametric Mann-Whitney U test in order to determine whether or not there exists a statistically significant difference between the hydrophobic energies of Type I and Type II protein groups. The “Analyze” tab was selected from the top menu bar, “Nonparametric Tests and Legacy Dialogs” were selected, and a “2 Independent Samples Test” was performed. Test and grouping

variables were organized and each group was defined as one and two, respectively. In the “Options” criteria, “Descriptives and MWU” were selected. Given $n_1=1118$, $n_2=155$, and the Sum of Ranks = 726967.50, the following formulas were used to derive the U test statistics for the hydrophobic energies of both Type I and Type II proteins:

$$U_1 = n_1 n_2 + \frac{n_1(n_1+1)}{2} - \text{Sum of Ranks}$$

$$U_2 = n_1 n_2 - (U_1)$$

The value that was selected to be compared to the U-critical value is the smaller of U_1 and U_2 ; thus, U_1 was retained.

Z Test of Hydrophobic Energies

In order to perform a Z test, the Z-test statistic of the hydrophobic energies was derived using the following formula:

$$\text{Standard Deviation} = \frac{\sqrt{(n_1 n_2)(n_1 + n_2 + 1)}}{12}$$

$$Z = \frac{U_1 - \frac{n_1 n_2}{2}}{\text{Standard Deviation}}$$

Monte Carlo Simulation of Normal Distribution of Shannon Entropies

A random number generator in Excel was used to generate 10,000 random transmembrane amino acid residue sequences. Shannon entropies for each sequence was calculated, and a frequency distribution of all sequence Shannon entropies was created in order to ensure that the Shannon entropies of the random sequences were normally distributed.

Shapiro Wilk Test of Gaussian Normality of Shannon Entropies

In order to determine if the assumption of normality required by the Student's T test was met by the Shannon entropies of Type I and Type II proteins, SPSS software was used to perform a Shapiro Wilk test. The "Analyze" tab was selected from the top menu bar, and the "Explore" function was selected. "Type" was moved to the "Factor List" space and "Shannon Entropy" was moved to the "Dependent List." The "Statistics" tab was opened and used to set the "Confidence Interval for the Mean" to 95%. Only the "Descriptives" box was checked. The "Plots" tab was opened and "Normality plots with tests" were checked. No changes were made to the "Options" criteria. As a supplement to the Shapiro Wilk test, histograms showing the frequency distributions of both Type I and Type II protein Shannon entropies were created in order to provide a secondary visual measure with which to assess the data. Histograms were created using Minitab.

Levene's Test of Equality of Variances of Shannon Entropies

A Levene's test of homogeneity of variances (SPSS) was used to determine if the assumptions of equal variances required by the Student's T test was met by the Shannon entropies of Type I and Type II proteins. The "Analyze" tab was selected from the top menu bar, the "Compare Means" function was selected, and a "One-Way ANOVA" was performed. No changes were made to the "Contrasts and Post Hoc criteria." Under "Options," "Homogeneity of Variances" was selected.

Mann-Whitney U Test of Shannon Entropies

Following the validation of the assumptions required by the parametric Student's T test, SPSS was used to perform a non-parametric Mann-Whitney U test in order to determine whether or not there exists a statistically significant difference between the

Shannon entropies of Type I and Type II protein groups. The “Analyze” tab was selected from the top menu bar, “Nonparametric Tests” and “Legacy Dialogs” were selected, and a “2 Independent Samples Test” was performed. Test and grouping variables were organized and each group was defined as one and two, respectively. In the “Options” criteria, “Descriptives and Mann-Whitney U test” were selected. Given $n_1=1118$, $n_2=155$, and the Sum of Ranks = 690642.50, the following formulas were used to derive the U-test statistics for the Shannon entropies of both Type I and Type II proteins:

$$U_1 = n_1 n_2 + \frac{n_1(n_1+1)}{2} - \text{Sum of Ranks}$$

$$U_2 = n_1 n_2 - (U_1)$$

The value that was selected to be compared to the U-critical value is the smaller of U_1 and U_2 ; thus, U_2 was retained.

Z Test of Shannon Entropies

In order to perform a Z test, the Z-test statistic of the Shannon entropies was derived using the following formula.

$$\text{Standard Deviation} = \frac{\sqrt{(n_1 n_2)(n_1 + n_2 + 1)}}{12}$$

$$Z = \frac{U_1 - \frac{n_1 n_2}{2}}{\text{Standard Deviation}}$$

Linear Regression of Hydrophobic Energies and Shannon Entropies

Shannon entropies of both Type I and Type II proteins were regressed against the transmembrane domain hydrophobic energies of both Type I and Type II proteins, respectively. Linear best fit lines and R^2 values were generated for each regression plot.

Chapter IV

RESULTS

Gibb's Free Energy Difference

The Gibb's free energy of Type I proteins was calculated to be 4.816 kJ/mol, and the Gibb's free energy of Type II proteins was calculated to be -4.816 kJ/mol. The total difference in electrical free energy ($\Delta\Delta G^\circ$) stability between and Type I and Type II proteins in the charged membrane field was calculated to be 9.63 kJ/mol using the following calculations:

$$\Delta G^\circ = \mu E$$

$$\Delta G_{\text{type1}}^\circ = [(0.5 e) \times (1.6 \times 10^{-19} \text{ C} / 1 e) \times (0.1 \text{ V}) \times (6.02 \times 10^{23} / \text{mol})] \times (10^{-3} \text{ kJ/J})$$

$$\Delta G_{\text{type1}}^\circ = 4.816 \text{ kJ/mol}$$

$$\Delta G_{\text{type2}}^\circ = -[(0.5 e) \times (1.6 \times 10^{-19} \text{ C} / 1 e) \times (0.1 \text{ V}) \times (6.02 \times 10^{23} / \text{mol})] \times (10^{-3} \text{ kJ/J})$$

$$\Delta G_{\text{type2}}^\circ = -4.816 \text{ kJ/mol}$$

$$\Delta\Delta G^\circ = \Delta G_{\text{type1}}^\circ - \Delta G_{\text{type2}}^\circ \quad \Delta\Delta G^\circ =$$

$$4.816 \text{ kJ/mol} - (-4.816 \text{ kJ/mol}) \quad \Delta\Delta G^\circ =$$

$$9.63 \text{ kJ/mol}$$

Frequency Distributions of Hydrophobic Energies

Histograms were constructed to provide preliminary and alternative visual assessment of the frequency distributions of hydrophobic energies for both groups of proteins (Figures 2 and 3). Type I mean hydrophobic energy was calculated to be 231.6 kJ/mol, while Type II mean hydrophobic energy was calculated to be 217.1 kJ/mol.

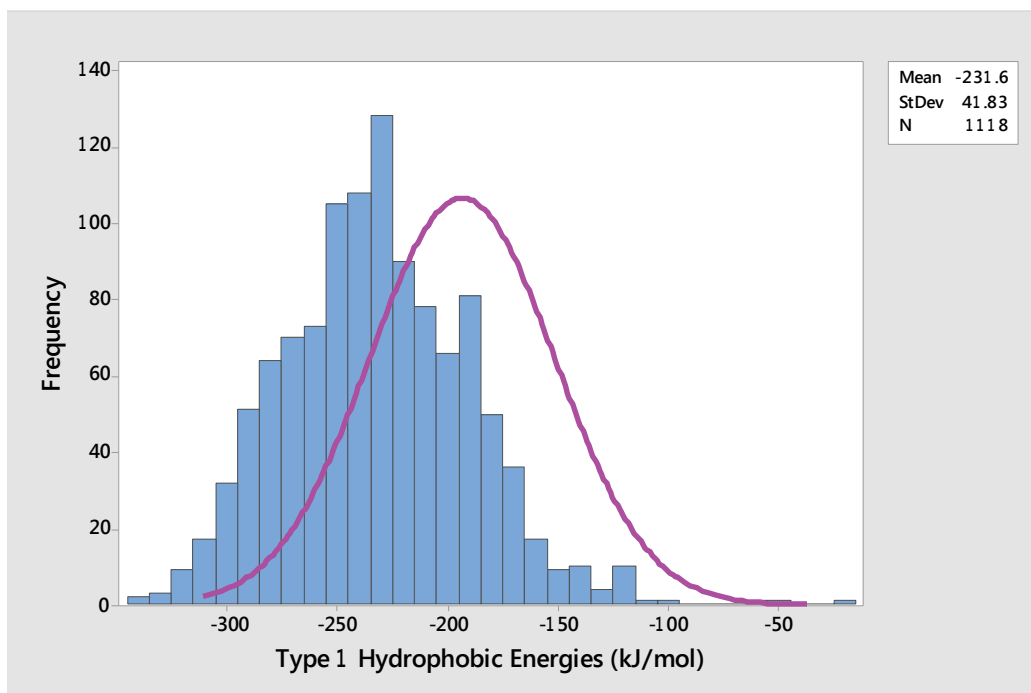


Figure 2. Frequency distribution of Type I TM protein hydrophobic energies

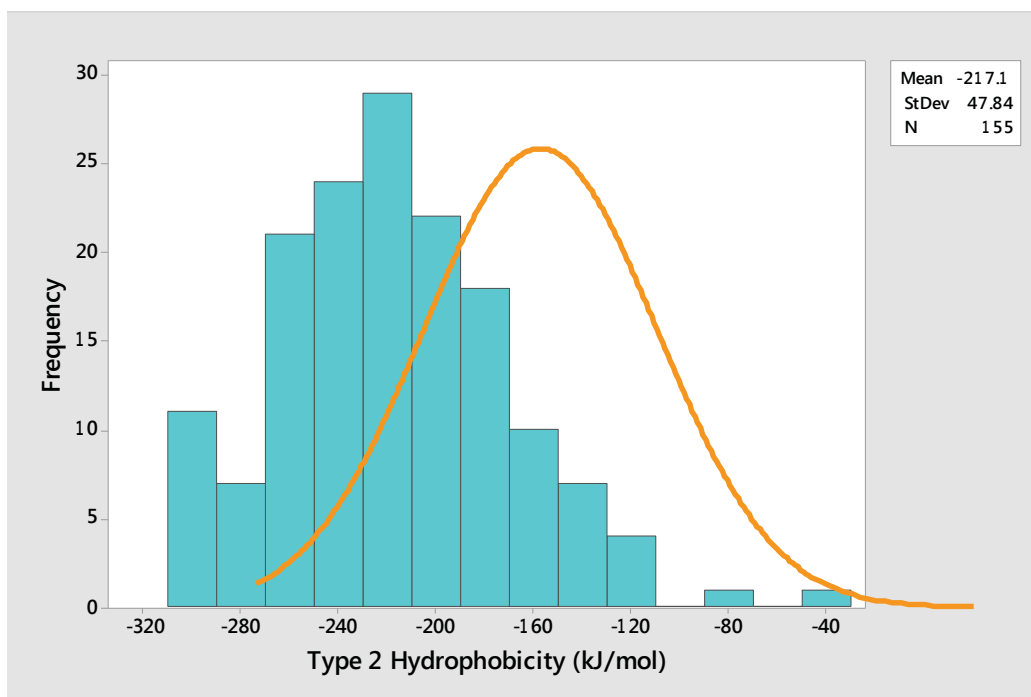


Figure 3. Frequency distribution of Type II TM protein hydrophobic energies

Mann-Whitney U Test of Hydrophobic Energies

The results of the Shapiro Wilk test show that both Type I and Type II protein groups violate the assumption of normality required by the Student's T test. This is indicated by the fact that the p values yielded by the Shapiro Wilk test using an $\alpha = 0.05$ for Type I and Type II protein groups are both significant ($p = 0.000$ and 0.017 , respectively). The results of the Levene's test show that the data for Type I and Type II protein groups violate the assumption of homogeneity of variances required by the Student's T test, given an alpha value of 0.05 . This is indicated by the fact that the p value yielded by the one-way ANOVA is less than 0.05 . The Levene's test yielded a p value of 0.038 . The descriptive statistics yielded a variance of 1749.9 and 2288.8 for Type I and Type II proteins, respectively. The results of the Mann-Whitney U test show that the mean ranks of Type I and Type II proteins are 650.24 and 541.51 , respectively (Table 1). The Mann-Whitney U Test that was performed in SPSS yielded a two-tailed asymptotic p value of 0.001 (Table 2), while the one-tailed test which was performed in Minitab yielded a significant p value of 0.0003 assuming a confidence level of 95% (Table 3).

$$U_1 = n_1 n_2 + \frac{n_1(n_1 + 1)}{2} - \text{Sum of Ranks}$$

$$U_2 = n_1 n_2 - (U_1)$$

$$U_1 = (1118)(155) + \frac{1118(1118+1)}{2} - 726967.50 \rightarrow 71843.5$$

$$U_2 = (1118)(155) - (71843.5) \rightarrow 101446.5$$

The value we compared to the U-critical value is the smaller of U_1 and U_2

Ranks				
	Type	N	Mean Rank	Sum of Ranks
Hydrophobicity	Type 1	1118	623.76	697364.50
	Type 2	155	732.49	113536.50
	Total	1273		

Table 1. Mean ranks of Type I and Type II TM protein hydrophobic energies

Test Statistics^a	
	Hydrophobicity y
Mann-Whitney U	71843.500
Wilcoxon W	83933.500
Z	-3.451
Asymp. Sig. (2-tailed)	.001

a. Grouping Variable: Type

Table 2. Asymptotic two-tailed p value of Mann-Whitney U test of hydrophobic energies

Mann-Whitney Test and CI: T1 Hydro, T2 Hydro		
	N	Median
T1 Hydrophobicity	1118	55.650
T2 Hydrophobicity	155	53.200
Point estimate for $\eta_1 - \eta_2$ is 3.200		
95.0 Percent CI for $\eta_1 - \eta_2$ is (1.400, 4.999)		
W = 726967.5		
Test of $\eta_1 = \eta_2$ vs $\eta_1 < \eta_2$ is significant at 0.0003		
The test is significant at 0.0003 (adjusted for ties)		

Table 3. Left-tailed p value of the Mann-Whitney U test of hydrophobic energies

Z Test of Hydrophobic Energies

The results of the two independent sample Z test on the mean hydrophobic energies of Type I and Type II proteins yielded a standard deviation of 2389.2 and a Z-test statistic of -3.4510, which corresponds to a p value of 0.0003, given $n_1=1118$, $n_2=155$, and $\alpha = 0.05$. This is in accordance with the results obtained by the Mann-Whitney U test.

$$\text{Standard Deviation} = \frac{\sqrt{(n_1 n_2)(n_1 + n_2 + 1)}}{12}$$

$$\text{Standard Deviation} = \frac{\sqrt{(1118 * 155)(1118 + 155 + 1)}}{12}$$

$$\text{Standard Deviation} = 4289.2$$

$$Z = \frac{U - \frac{n_1 n_2}{2}}{\text{Standard Deviation}}$$

$$Z = \frac{71843.5 - \frac{(1118)(155)}{2}}{4289.2} \rightarrow -3.4510$$

Frequency Distributions of Shannon Entropies

Histograms were constructed to provide preliminary and alternative visual assessment of the frequency distributions for both groups of proteins (Figures 4 and 5). Type I mean Shannon entropy was calculated to be 2.560 bits, while Type II mean Shannon entropy was calculated to be 2.68 bits.

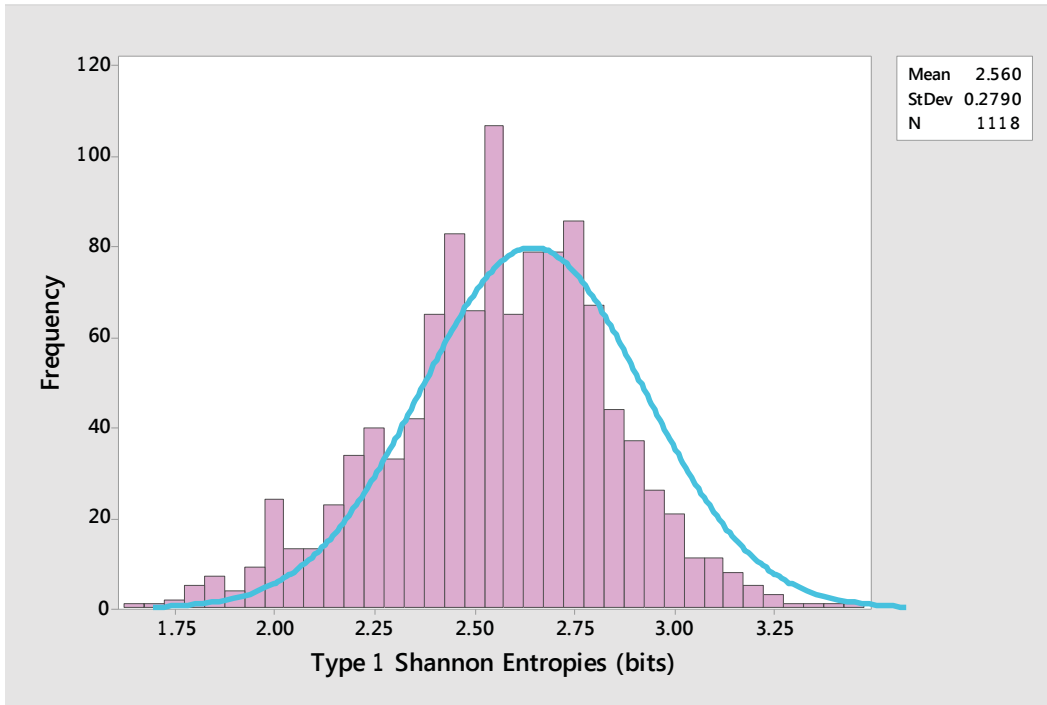


Figure 4. Frequency distribution of Type I TM protein Shannon entropies

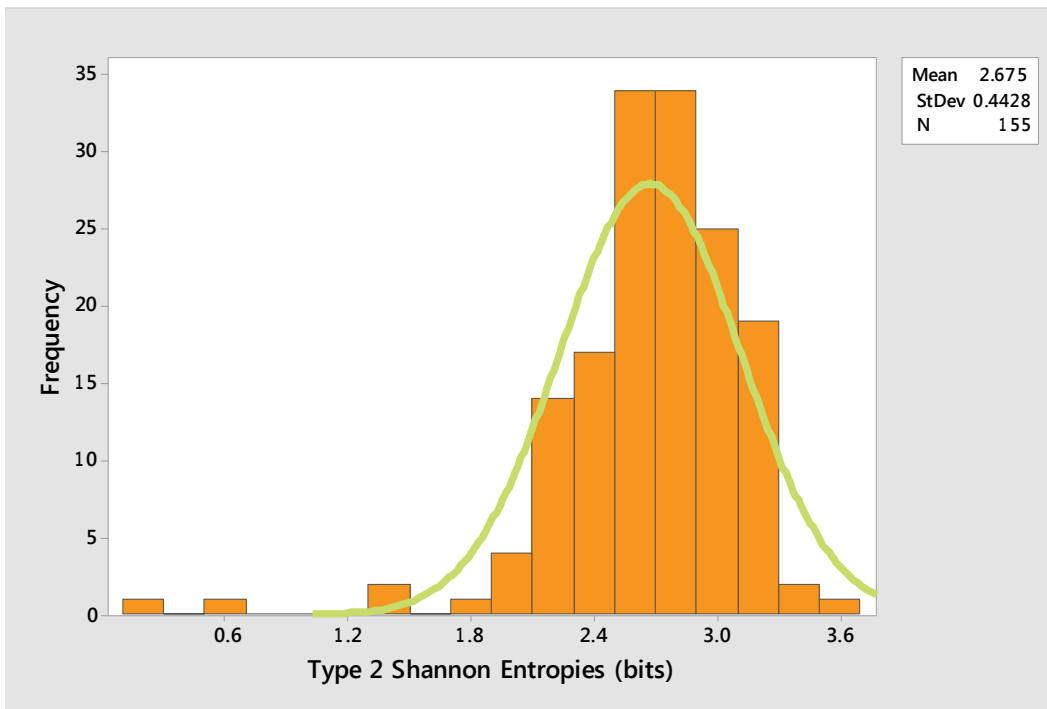


Figure 5. Frequency distribution of Type II TM protein Shannon entropies

Mann-Whitney U Test of Shannon Entropies

The results of the Shapiro Wilk test show that both Type I and Type II protein groups violate the assumption of normality required by the Student's T test. This is indicated by the fact that the p values yielded by the Shapiro Wilk test using $\alpha = 0.05$ for Type I and Type II protein groups are both significant ($p = 0.000$ and 0.000 , respectively). The results of the Levene's test show that the data for Type I and Type II protein groups violate the assumption of homogeneity of variances required by the Student's T test, given an alpha value of 0.05. This is indicated by the fact that the p value yielded by the one way ANOVA is less than 0.05. The Levene's test yielded a p-value of 0.000. The descriptive statistics yielded a variance of 0.078 and 0.196 for Type I and Type II proteins, respectively. The results of the Mann-Whitney U test show that the mean ranks of Type I and Type II Shannon entropies are 617.75 and 775.86 respectively (Table 4). The Mann-Whitney U test that was performed in SPSS yielded a two-tailed asymptotic p value of 0.000 (Table 5), while the one-tailed test which was performed in Minitab yielded a p value of significant p value of 0.000 assuming a confidence level of 95% (Table 6).

$$U_1 = n_1 n_2 + \frac{n_1(n_1 + 1)}{2} - \text{Sum of Ranks}$$

$$U_2 = n_1 n_2 - (U_1)$$

$$U_1 = (1118)(155) + \frac{1118(1118+1)}{2} - 690642.50 \rightarrow 108168.5$$

$$U_2 = (1118)(155) - (108168.5) \rightarrow 65121.5$$

The value we compared to the U-critical value is the smaller of U_1 and U_2

Ranks				
	Type	N	Mean Rank	Sum of Ranks
ShannonEntropy	Type 1	1118	617.75	690642.50
	Type 2	155	775.86	120258.50
	Total	1273		

Table 4. Mean ranks of Type I and Type II TM protein Shannon entropies

Test Statistics ^a	
	ShannonEntropy
Mann-Whitney U	65121.500
Wilcoxon W	690642.500
Z	-5.018
Asymp. Sig. (2-tailed)	.000

a. Grouping Variable: Type

Table 5. Asymptotic two-tailed p value of Mann-Whitney U test of Shannon entropies

Mann-Whitney Test and CI: T1 SE, T2 Hydro		
	N	Median
T1 Shannon Entropies	1118	2.5708
T2 Shannon Entropies	155	2.7200
Point estimate for $\eta_1 - \eta_2$ is -0.1438		
95.0 Percent CI for $\eta_1 - \eta_2$ is (-0.1970, -0.0889)		
W = 690642.5		
Test of $\eta_1 = \eta_2$ vs $\eta_1 < \eta_2$ is significant at 0.0000		
The test is significant at 0.0000 (adjusted for ties)		

Table 6. Left-tailed p value of Mann-Whitney U test of Shannon entropies

Z Test of Shannon Entropies

The results of the two independent sample Z test on the mean Shannon entropies of Type I and Type II proteins yielded a standard deviation of 4289.2 and a Z-test statistic of -5.018, which corresponds to a p value of 0.0000, given $n_1=1118$, $n_2=155$, and $\alpha = 0.05$. This is in accordance with the results obtained by the Mann-Whitney U test.

$$\text{Standard Deviation} = \frac{\sqrt{(n_1 n_2)(n_1 + n_2 + 1)}}{12}$$

$$\text{Standard Deviation} = \frac{\sqrt{(1118 * 155)(1118 + 155 + 1)}}{12}$$

$$\text{Standard Deviation} = 4289.2$$

$$Z = \frac{U - \frac{n_1 n_2}{2}}{\text{Standard Deviation}}$$

$$Z = \frac{65121.5 - \frac{(1118)(155)}{2}}{4289.2} \rightarrow -5.018$$

Shannon Entropy as a Function of Hydrophobic Energy

Shannon entropies of Type I proteins were plotted against hydrophobic energies of Type I proteins, and an R^2 of 0.221 was obtained (Figure 6). The residual sum of squares was computed to be 67.7 (Table 7). Shannon entropies of Type II proteins were plotted against hydrophobic energies of Type II proteins, and R^2 of 0.232 was obtained (Figure 7). The residual sum of squares was calculated to be 23.2 (Table 8).

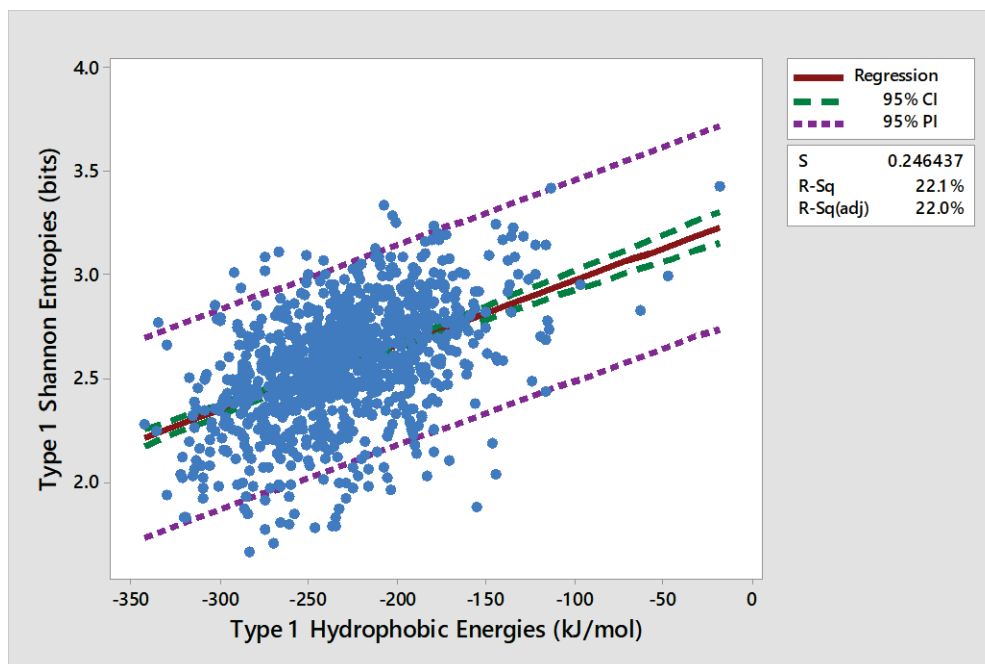


Figure 6. Linear regression plot of Type I Shannon entropies as a function of Type I TM protein hydrophobic energies

Model Summary

Model	R	R Square	Adjusted R Square	Std. Error of the Estimate
1	.470 ^a	.221	.220	.24644

a. Predictors: (Constant), VAR00001

ANOVA^a

Model		Sum of Squares	df	Mean Square	F	Sig.
1	Regression	19.187	1	19.187	315.935	.000 ^b
	Residual	67.776	1116	.061		
	Total	86.963	1117			

a. Dependent Variable: VAR00002

b. Predictors: (Constant), VAR00001

Table 7. ANOVA table of linear regression analysis of Type I Shannon entropies plotted as a function of Type I hydrophobic energies

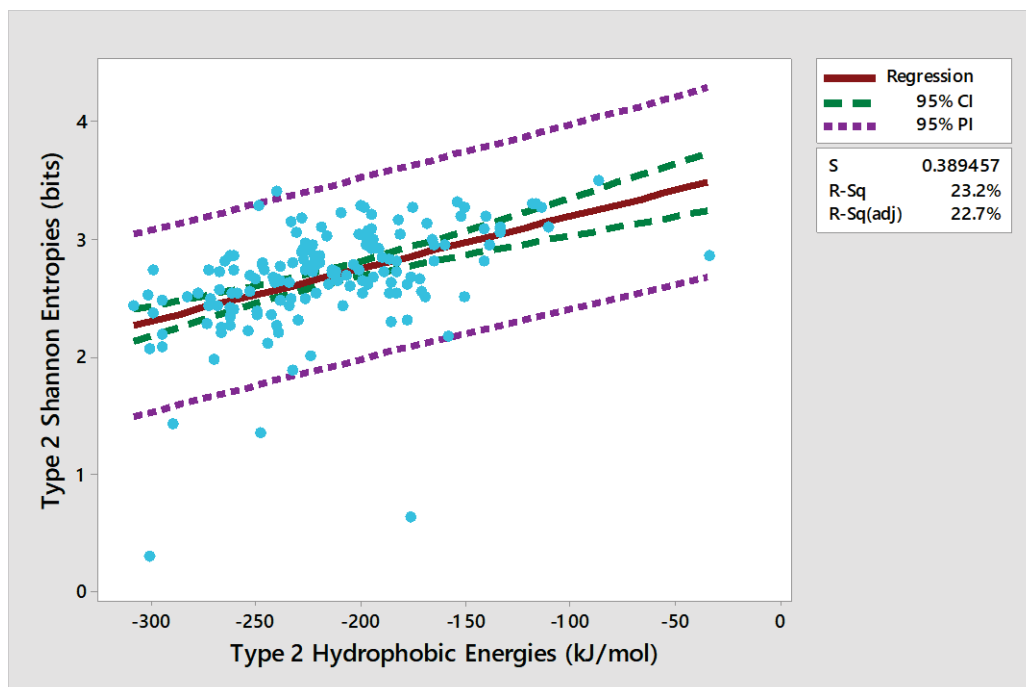


Figure 7. Linear regression analysis of Type II Shannon entropies as a function of Type II TM protein hydrophobic energies

Model Summary

Model	R	R Square	Adjusted R Square	Std. Error of the Estimate
1	.481 ^a	.232	.227	.38946

a. Predictors: (Constant), VAR00004

ANOVA^a

Model		Sum of Squares	df	Mean Square	F	Sig.
1	Regression	6.994	1	6.994	46.112	.000 ^b
	Residual	23.206	153	.152		
	Total	30.201	154			

a. Dependent Variable: VAR00005

b. Predictors: (Constant), VAR00004

Table 8. ANOVA table of linear regression analysis of Type II Shannon entropies plotted as a function of Type II hydrophobic energies

Functional Classification

The relative abundances of Type I (striped) and Type II (dotted) proteins categorized by biological, molecular, and enzymatic function. Among Type I proteins (n = 1118), those that functioned in immune pathways were the most abundant, followed closely by those that functioned exclusively as receptors (Figure 8). Similarly, among Type II TM proteins (n = 155), those that functioned in immune pathways were the most abundant, followed by enzymes (Figure 8).

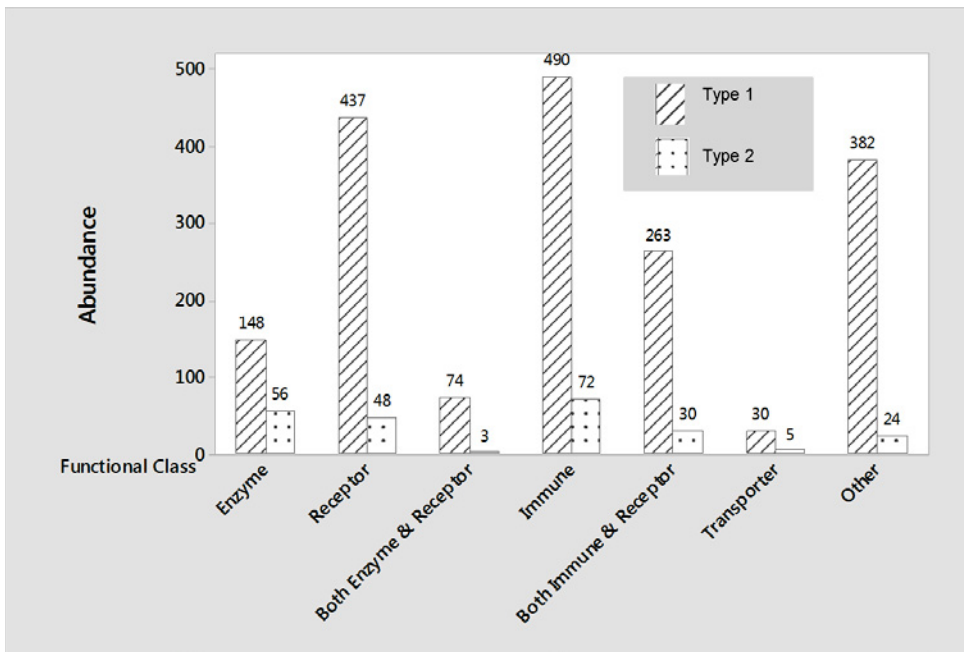


Figure 8. Classification of Protein Function

Chapter V

DISCUSSION

Hydrophobic Energy Compensation

The overall Gibb's free energy difference between Type I and Type II proteins was calculated to be approximately 9.63 kJ/mol. The mean hydrophobic energy yielded by descriptive statistics was calculated to be 231.6 kJ/mol for Type I proteins and 217.1 kJ/mol for Type II proteins. The difference in the mean hydrophobic energies between the two types of proteins was calculated to be 14.5 kJ/mol. Thus, the difference in hydrophobic energies appears to exceed the free energy difference between Type I and Type II proteins. Although hydrophobic energy appears to overcompensate for the energy disparity between Type I and Type II proteins, this observation may also be attributed to energy interactions among a variety of energetic contributors, but more research is needed in order to elucidate such factors and their specific roles in energy compensation.

Z Test of Transmembrane Domain Hydrophobic Energies

The results of both the Z test and the Mann-Whitney U test of hydrophobic energies indicate that the mean hydrophobic energies of Type I proteins are significantly greater than the mean hydrophobic energies of Type II proteins ($p = 0.0003$). The Z-test statistic for the hydrophobic energies was $|-3.4510| > 1.96$ for $\alpha = 0.05$, indicating rejection of the null hypothesis. The mean rank of Type I protein hydrophobic energies was calculated to be 650.24, while the mean rank of Type II protein hydrophobic energies

was calculated to be 541.51. These results indicate significant disparities in the hydrophobic energies exhibited by Type I and Type II transmembrane domains. Given the estimated differences between the stabilities of Type I and Type II transmembrane proteins and the tendency of thermodynamic systems to achieve the lowest energy state possible, it may be hypothesized that such differences in hydrophobic energies may have arisen due to the energetic disadvantage of Type I protein orientation. The selective pressures exerted by energetically unfavorable interactions between the charged dipole termini and the membrane field potential may impose evolutionary constraints on the hydrophobic character of transmembrane domains belonging to bitopic proteins, and perhaps those of polytopic proteins. It is possible that increased selection of transmembrane proteins exhibiting greater hydrophobic character may serve as an adaptive response to the subsequent energy disadvantages encountered by the globular termini of Type I proteins. Admittedly, understanding of the mechanisms underlying this process is still in its infancy, and more research is required to fully elucidate the evolutionary link between transmembrane protein selection and the hydrophobicities of their transmembrane domains.

Z Test of Transmembrane Domain Shannon Entropies

The results of both the Z test and the Mann-Whitney U test of Shannon entropies show that the mean information entropies of Type I transmembrane proteins are significantly lower than the Shannon entropies of Type II transmembrane proteins ($p = 0.000$). The Z-test statistic for Shannon entropies was $|-5.018| > 1.96$ for $\alpha = 0.05$, indicating rejection of the null hypothesis. The mean rank of Type I transmembrane protein Shannon entropies was calculated to be 617.75, while the mean rank of Type II

transmembrane protein Shannon entropies was calculated to be 775.86. These results indicate that the maximum possible states that can be assumed by transmembrane domains of Type I proteins are much lower than the maximum possible states that can be assumed by Type II proteins. In addition, the amount of information that is needed to describe the state of Type I protein transmembrane domains is much lower than that needed to describe the state of Type II protein transmembrane domains. These disparities may be due to increased hydrophobicity in Type I protein transmembrane domains relative to their Type II counterparts. This phenomenon may be attributed to the biochemical and stereochemical constraints that arise from Type I proteins' evolutionary need to assume a lower hydrophobic energy in order to compensate for free energy disadvantages. Specifically, the tendency of Type I proteins to exhibit greater hydrophobicities in order to optimize energetic favorability may require the composition of their transmembrane domains to be dominated by hydrophobic residues or site-specific burial of hydrophilic side chains.

Linear Regression Analysis of Shannon Entropy as a Function of Hydrophobic Energy

The results of the linear regression analysis for Type I proteins reveal a weak correlation between hydrophobic energy and Shannon entropy ($R^2 = 0.221$, $RSS = 67.7$). Similar results were obtained for Type II proteins ($R^2 = 0.232$, $RSS = 23.2$). The weak correlation between these two parameters indicates that the information entropies of transmembrane domains are not directly proportional to transmembrane domain hydrophobic energies. This means that transmembrane domain hydrophobicities are not the sole determinants of transmembrane domain entropies. Given the results, it may be hypothesized that overall entropies may actually be a product of multiple interactions

among several energy inputs. Whether these interactions are additive or synergistic is unclear, and more research is needed in order to identify other forces that may influence transmembrane domain entropies.

Functional Classification

It appears that differences in hydrophobic energy may not directly influence protein functional roles. This is indicated by the fact that the majority of both Type I and Type II protein groups were found to function in immune pathways. For Type I proteins, the second most abundant functional role was found to be receptors. For Type II proteins, the second most abundant functional role was enzymes. It is unclear whether these differences may be linked to disparities in hydrophobic energies of transmembrane domains. More research is required to identify any specific correlations between hydrophobic energy and protein function.

Summary

Thermodynamics is the guiding principal that governs all change. Examining the thermodynamic mechanisms underlying transmembrane protein stability is critical to gaining a fundamental understanding of transmembrane protein energetics within lipid mediums and the evolutionary mechanisms that regulate their relative populations. This study exposes inherent differences between the hydrophobicities and the Shannon entropies exhibited by two broad categories of transmembrane proteins. The findings of this study suggest that transmembrane protein insertion is not a strictly stochastic process but ultimately one that is selectively governed by biophysical determinants. This study also reveals that transmembrane domain entropies are not a direct result of hydrophobic

free energies, but may be attributed to other energetic modulators, although these specific agents have yet to be identified.

Many diseases depend upon pathways involving transmembrane proteins and their functional roles. Certain diseases may interfere with transmembrane protein function and disrupt normal pathways, or they may simply use transmembrane proteins to elicit pathogenicity. Biomedical engineering of appropriate drugs depends very much on a comprehensive understanding of transmembrane protein stability. By understanding the thermodynamic landscape of transmembrane protein stability, researchers can more effectively design disease-combatting drugs in order to improve the quality of human health, and, in turn, the quality of human life.

REFERENCES

- Agnati, L.F., Guidolin, D., Genedani, S., Ferre, S., Bigiani, A., Woods, A.S., & Fuxe, K. (2005). How proteins come together in the plasma membrane and function in macromolecular assemblies: Focus on receptor mosaics. *Journal of Molecular Neuroscience*, 26(2), 133-154. doi:10.1385/JMN:26:2-3:133.
- Albers, R.W. (1999). Membrane proteins. In Siegel, G.J., Agranoff, B.W., Albers, R.W., Fisher, S.K., & Uhler, M.D. (Eds.), *Basic neurochemistry: Molecular, cellular and medical aspects* (6th ed.). Philadelphia: Lippincott-Raven.
- Andreu-Fernandez, V., Sancho, M., Genoves, A., Lucendo, E., Todt, F., Lauterwasser, J., Funk, K., Jahreis, G., Perez-Paya, E., Mingarro, I., Edlich, F., & Orzaez, M. (2016). Bax transmembrane domain interacts with prosurvival Bcl-2 proteins in biological membranes. *Proceedings of the National Academy of Sciences of the United States of America*, 114(2), 310-315. doi: 10.1073/pnas.1612322114.
- Berg, K.H., Straume, D., & Havarstein, L.S. (2014). The function of the transmembrane and cytoplasmic domains of pneumococcal penicillin-binding proteins 2x and 2b extends beyond that of simple anchoring devices. *Microbiology*, 160, 1585-1598. doi: 10.1099/mic.0.078535-0.
- Brady, S.T., Siegel, G.J., Albers, R.W., & Price, D.L. (2012). *Basic neurochemistry* (Eighth Ed.). Waltham, MA: Elsevier.
- Buck, T.M., Jordahl, A.S., Yates, M.E., Preston, M., Cook, E., Kleyman, T.R., & Brodsky, J.L. (2016). Interactions between intersubunit transmembrane domains regulate the chaperone dependent degradation of an oligomeric membrane protein. *The Biochemical Journal*. doi: 10.1042/BCJ20160760.
- Chothia, C. (1976). The nature of the accessible and buried surfaces in proteins. *Journal of Molecular Biology*, 105(1), 1-12. doi:10.1016/0022-2836(76)90191-1.
- Cole, B. J., & Bystroff, C. (2009). Alpha helical crossovers favor right-handed supersecondary structures by kinetic trapping: The phone cord effect in protein folding. *Protein Science: A Publication of the Protein Society*, 18(8), 1602–1608. doi:10.1002/pro.182
- Cooper, G.M. (2000). Structure of the plasma membrane. In *The cell: A molecular approach* (2nd ed.). Sunderland, MA: Sinauer Associates.
- de Jesus, A.J., & Allen, T.W. (2013). The determinants of hydrophobic mismatch response for transmembrane helices. *Biochimica et Biophysica Acta (BBA)*, 1828, 851–863.

- Deol, S. S., Bond, P. J., Domene, C., & Sansom, M. S. P. (2004). Lipid-Protein interactions of integral membrane proteins: A comparative simulation study. *Biophysical Journal*, 87(6), 3737–3749. doi:10.1529/biophysj.104.048397
- Dror, R. O., Pan, A. C., Arlow, D. H., Borhani, D. W., Maragakis, P., Shan, Y., Xu, H., & Shaw, D. E. (2011). Pathway and mechanism of drug binding to G-protein-coupled receptors. *Proceedings of the National Academy of Sciences of the United States of America*, 108(32), 13118–13123. doi:10.1073/pnas.1104614108
- Goder, V., & Spiess, M. (2001). Topogenesis of membrane proteins: Determinants and dynamics. *FEBS Letters*, 504(3), 87-93. doi:10.1016/S0014-5793(01)02712-0
- Godfroy, J. I., Roostan, M., Moroz, Y. S., Korendovych, I. V., & Yin, H. (2012). Isolated toll-like receptor transmembrane domains are capable of oligomerization. *PLoS ONE Journal*, 7(11). doi.org/10.1371/journal.pone.0048875
- Guerriero, C. J., Reutter, K.R., Augustine, A. A., Preston, G. M., Weiberth, K. F., Mackie, T. D., Cleveland-Rubeor, H.C., Bethel, N.P., Callenberg, K.M., Nakatsukasa, K., Grabe, M., & Brodsky, J. L. (2017). Transmembrane helix hydrophobicity is an energetic barrier during the retrotranslocation of integral membrane ERAD substrates. *Molecular Biology of the Cell*, 28(15), 2076–2090. doi:10.1091/mbc.E17-03-0184
- Gurtovenko A.A., & Vattulainen, I. (2008). Membrane potential and electrostatics of phospholipid bilayers with asymmetric transmembrane distribution of anionic lipids. *Journal of Physical Chemistry and Biology*, 112, 4629–4634.
- Haltia, T., & Freire, E. (1995). Forces and factors that contribute to the structural stability of membrane-proteins. *Biochimica et Biophysica Acta (BBA) - Bioenergetics*, 1228(1), 1–27. doi:10.1016/0005-2728(94)00161-W.
- Hine, J., & Mookerjee, P.K. (1975). Structural effects on rates and equilibria. XIX. Intrinsic hydrophilic character of organic compounds. Correlations in terms of structural contributions. *The Journal of Organic Chemistry*, 40(3), 292-298. doi:10.1021/jo00891a006.
- Holt, A., Koehorst, R. B. M., Rutters-Meijneke, T., Gelb, M. H., Rijkers, D. T. S., Hemminga, M. A., & Killian, J. A. (2009). Tilt and rotation angles of a transmembrane model peptide as studied by fluorescence spectroscopy. *Biophysical Journal*, 97(8), 2258–2266. doi:10.1016/j.bpj.2009.07.042
- Hu, J., Asbury, T., Achuthan, S., Li, C., Bertram, R., Quine, J. R., Fu, R., & Cross, T. A. (2007). Backbone structure of the amantadine-blocked *trans*-membrane domain M2 proton channel from Influenza A virus. *Biophysical Journal*, 92(12), 4335–4343. doi.org/10.1529/biophysj.106.090183

- Hubert, P., Sawma, P., Duneau, J.P., Khao, J., Henin, J., Bagnard, D., & Sturgis, J. (2010). Single-spanning transmembrane domains in cell growth and cell-cell interactions. More than meets the eye? *Cell Adhesion & Migration*, 4(2), 313-324. doi:10.4161/cam.4.2.12430
- Jia, H., Liggins, J. R., & Chow, W. S. (2014). Entropy and biological systems: Experimentally-investigated entropy-driven stacking of plant photosynthetic membranes. *Scientific Reports*, 4, 4142. <http://doi.org/10.1038/srep04142>
- Kaykas, A., Worringer, K., & Sugden, B. (2002). LMP-1's transmembrane domains encode multiple functions required for LMP-1's efficient signaling. *Journal of Virology*, 76(22), 11551-11560. doi: 10.1128/JVI.76.22.11551-11560.2002.
- Kim, T., & Im, W. (2010). Revisiting hydrophobic mismatch with free energy simulation studies of transmembrane helix tilt and rotation. *Biophysical Journal*, 99(1), 175–183. doi.org/10.1016/j.bpj.2010.04.015
- Kyte, J., & Doolittle, R.F. (1982). A simple method for displaying the hydrophobic character of a protein. *Journal of Molecular Biology*, 157, 105–132. doi: 10.1016/0022-2836(82)90515-0.
- Lee, A.G. (2004). How lipids affect the activities of integral membrane proteins. *Biochimica et Biophysica Acta (BBA)*, 1666(1-2), 62–87. doi:10.1016/j.bbamem.2004.05.012.
- Mo, X, Yang, R., & Tao, Y. (2012). Functions of transmembrane domain 3 of human melanocortin-4 receptor. *Journal of Molecular Endocrinology*, 49221-235. doi: 10.1530/JME-12-0162.
- Moran, L.A., Horton, R.A., Scrimgeour, G., & Perry, M. (2011). *Principles of biochemistry* (5th Ed.). Boston, MA: Pearson.
- Nagle, J. F., & Tristram-Nagle, S. (2000). Lipid bilayer structure. *Current Opinion in Structural Biology*, 10(4), 474–480.
- Opella, S. J., & Marassi, F. M. (2004). Structure determination of membrane proteins by NMR spectroscopy. *Chemical Reviews*, 104(8), 3587–3606. doi:10.1021/cr0304121
- Park, S.H., & Opella, S. (2005). Tilt angle of a trans-membrane helix is determined by hydrophobic mismatch. *Journal of Molecular Biology*, 350(2), 310-8. doi:10.1016/j.jmb.2005.05.004.
- Párkányi, C. (1998). *Theoretical and Computational Organic Chemistry* (1st Ed.). Amsterdam, Netherlands: Elsevier Science.

- Peters, C., & Elofsson, A. (2014). Why is the biological hydrophobicity scale more accurate than earlier experimental hydrophobicity scales? *Proteins*, *82*, 2190–2198.
- Pike, J.L. (2003). Lipid rafts bringing order to chaos. *The Journal of Lipid Research*, *44*, 644–667. doi: 10.1194/jlr.R200021-JLR200
- Punta, M., Forrest, L. R., Bigelow, H., Kernytsky, A., Liu, J., & Rost, B. (2007). Membrane protein prediction methods. *Methods*, *41*(4), 460–474. doi:10.1016/j.ymeth.2006.07.026
- Simon, S.A., Advani, S., & McIntosh, T.J. (1995). Temperature dependence of the repulsive pressure between phosphatidylcholine bilayers. *Biophysical Journal*, *69*, 1473–1483.
- Simons, K., & Sampaio, J. L. (2011). Membrane organization and lipid rafts. *Cold Spring Harbor Perspectives in Biology*, *3*(10). doi:10.1101/cshperspect.a004697
- Van Klompenburg, W., Nilsson, I., von Heijne, G., & de Kruijff, B. (1997). Anionic phospholipids are determinants of membrane protein topology. *The EMBO Journal*, *16*(14), 4261–4266.
- VanderSpek, J.C., Mindell, J.A., Finkelstein, A., & Murphy, J.R. (1993). Structure/Function analysis of the transmembrane domain of DAB389-Interleukin-2, an Interleukin-2 receptor-targeted fusion toxin. *The Journal of Biological Chemistry*, *268*(16), 12077–12082.
- Wolfenden, R.V., Cullis, P.M., & Southgate, C.C.F. (1979). Water, protein folding, and the genetic code. *Science*, *206*(4418), 575–577.
- Yang, N. J., & Hinner, M. J. (2015). Getting across the cell membrane: An overview for small molecules, peptides, and proteins. *Methods in Molecular Biology*, *1266*, 29–53. doi:10.1007/978-1-4939-2272-7_3
- Yin, H., & Flynn, A. D. (2016). Drugging membrane protein interactions. *Annual Review of Biomedical Engineering*, *18*, 51–76. doi:10.1146/annurev-bioeng-092115-025322
- Zhou, C., Zheng, Y., & Zhou, Y. (2004). Structure prediction of membrane proteins. *Genomics, Proteomics & Bioinformatics*, *2*(1), 1–5. doi:10.1016/S1672-0229(04)02001-7
- Zvilning, M., Kochva, U., & Arkin, I.T. (2007). How important are transmembrane helices of bitopic membrane proteins? *Biochimica et Biophysica Acta (BBA) – Biomembranes*, *1768*(3), 387–392.

APPENDIX A:

Kyte and Doolittle Amino Acid Hydrophobicity Indices

APPENDIX A: Kyte and Doolittle Amino Acid Hydrophobicity Indices

Ala: 1.800

Arg: -4.500

Asn: -3.500

Asp: -3.500

Cys: 2.500

Gln: -3.500

Glu: -3.500

Gly: -0.400

His: -3.200

Ile: 4.500

Leu: 3.800

Lys: -3.900

Met: 1.900

Phe: 2.800

Pro: -1.600

Ser: -0.800

Thr: -0.700

Trp: -0.900

Tyr: -1.300

Val: 4.200

APPENDIX B:

Type I Protein Hydrophobic Energies and Shannon Entropies

APPENDIX B: Type I Protein Hydrophobic Energies and Shannon Entropies

Uniprot ID	Protein Name	Hydrophobic Energy (kJ/mol)	Shannon Entropy (bits)
Q04771	Activin receptor type-1	285.35	2.559
P36896	Activin receptor type-1B	314.22	2.255
Q8NER5	Activin receptor type-1C	212.97	3.082
P27037	Activin receptor type-2A	200.83	3.252
Q13705	Activin receptor type-2B	184.93	2.834
Q15109	Advanced glycosylation end product-...	192.88	2.451
Q9UM73	ALK tyrosine kinase receptor	206.27	2.895
Q7Z6M3	Allergin-1	275.31	2.211
Q16586	Alpha-sarcoglycan	242.25	2.009
Q86WK6	Amphoterin-induced protein 1	194.14	2.856
Q86SJ2	Amphoterin-induced protein 2	199.16	2.710
Q86WK7	Amphoterin-induced protein 3	196.65	2.492
P05067	Amyloid beta A4 protein	265.68	2.674
P51693	Amyloid-like protein 1	196.65	2.610
Q06481	Amyloid-like protein 2	288.28	2.717
Q02763	Angiopoietin-1 receptor	212.55	2.895
P12821	Angiotensin-converting enzyme	178.24	2.686
Q9BYF1	Angiotensin-converting enzyme 2	278.65	2.250
Q9H6X2	Anthrax toxin receptor 1	261.50	1.787
P58335	Anthrax toxin receptor 2	260.66	2.559
A6NF34	Anthrax toxin receptor-like	183.26	2.375
P15813	Antigen-presenting glycoprotein CD1...	242.25	2.623
Q16671	Anti-Muellerian hormone type-2 rece...	274.47	1.765
Q6UXC1	Apical endosomal glycoprotein	221.33	2.331
P16066	Atrial natriuretic peptide receptor...	216.73	2.558
P20594	Atrial natriuretic peptide receptor...	168.20	2.722
P17342	Atrial natriuretic peptide receptor...	189.95	2.799
O75882	Attractin	211.29	2.371
Q5VV63	Attractin-like protein 1	211.29	2.371
Q7Z6A9	B- and T-lymphocyte attenuator	188.70	2.262
P50895	Basal cell adhesion molecule	247.27	2.246
P35613	Basigin	217.99	2.833
P11912	B-cell antigen receptor complex-ass...	208.36	2.894
P40259	B-cell antigen receptor complex-ass...	253.13	2.376
P20273	B-cell receptor CD22	206.27	2.676
Q16620	BDNF/NT-3 growth factors receptor	280.33	2.661
P56817	Beta-secretase 1	221.33	2.841
Q9Y5Z0	Beta-secretase 2	251.04	2.686
Q9Y6X5	Bis(5'-adenosyl)-triphosphatase ENP...	250.62	2.815
P15391	B-lymphocyte antigen CD19	203.34	3.033
Q13145	BMP and activin membrane-bound inhi...	251.46	2.570

P36894	Bone morphogenetic protein receptor...	243.51	2.965
O00238	Bone morphogenetic protein receptor...	257.32	2.641
Q13873	Bone morphogenetic protein receptor...	253.13	2.627
Q9BWV1	Brother of CDO	247.27	2.644
Q13410	Butyrophilin subfamily 1 member A1	241.84	3.065
Q7KYR7	Butyrophilin subfamily 2 member A1	244.76	2.790
Q8WVV5	Butyrophilin subfamily 2 member A2	246.02	2.757
O00481	Butyrophilin subfamily 3 member A1	124.26	2.484
P78410	Butyrophilin subfamily 3 member A2	176.56	2.567
O00478	Butyrophilin subfamily 3 member A3	157.32	2.669
A8MVZ5	Butyrophilin-like protein 10	211.29	2.936
Q6UXE8	Butyrophilin-like protein 3	238.07	2.669
Q6UX41	Butyrophilin-like protein 8	196.65	2.514
Q6UXG8	Butyrophilin-like protein 9	214.64	2.324
P12830	Cadherin-1	283.26	1.655
Q9Y6N8	Cadherin-10	321.75	2.119
P55287	Cadherin-11	317.57	2.495
P55289	Cadherin-12	334.72	2.764
P55291	Cadherin-15	284.93	1.843
O75309	Cadherin-16	217.15	2.589
Q12864	Cadherin-17	261.50	2.474
Q13634	Cadherin-18	329.70	2.655
Q9H159	Cadherin-19	270.70	2.421
P19022	Cadherin-2	313.80	2.345
Q9HBT6	Cadherin-20	298.32	2.269
Q9UJ99	Cadherin-22	311.29	2.159
Q9H251	Cadherin-23	257.73	2.338
Q86UP0	Cadherin-24	266.94	2.453
P22223	Cadherin-3	310.03	1.917
P55283	Cadherin-4	289.11	2.653
P33151	Cadherin-5	270.70	2.407
P55285	Cadherin-6	297.48	2.305
Q9ULB5	Cadherin-7	283.68	2.416
P55286	Cadherin-8	302.92	2.347
Q9ULB4	Cadherin-9	314.64	2.054
Q8IXH8	Cadherin-like protein 26	232.21	2.213
Q9BYE9	Cadherin-related family member 2	260.24	2.628
Q6ZTQ4	Cadherin-related family member 3	247.69	2.316
A6H8M9	Cadherin-related family member 4	197.48	2.365
Q9HBB8	Cadherin-related family member 5	235.14	1.822
Q9UQC9	Calcium-activated chloride channel ...	230.96	2.820
O94985	Calsyntenin-1	264.43	2.628
Q9H4D0	Calsyntenin-2	259.41	2.739
Q9BQT9	Calsyntenin-3	271.54	2.567
O43570	Carbonic anhydrase 12	261.08	2.584
Q9ULX7	Carbonic anhydrase 14	228.03	2.667

Q16790	Carbonic anhydrase 9	211.71	2.725
O75976	Carboxypeptidase D	176.98	3.165
P13688	Carcinoembryonic antigen-related ce...	298.32	2.399
Q7Z692	Carcinoembryonic antigen-related ce...	200.41	2.529
Q6UY09	Carcinoembryonic antigen-related ce...	212.55	2.919
Q3KPI0	Carcinoembryonic antigen-related ce...	265.68	2.437
P40198	Carcinoembryonic antigen-related ce...	258.15	2.447
O75871	Carcinoembryonic antigen-related ce...	258.15	2.447
Q86XM0	Cation channel sperm-associated pro...	212.13	2.601
Q6ZRH7	Cation channel sperm-associated pro...	233.47	2.645
Q6UWJ8	CD164 sialomucin-like 2 protein	197.48	2.569
Q13740	CD166 antigen	246.86	2.526
Q99467	CD180 antigen	317.15	2.188
Q15762	CD226 antigen	234.30	2.417
P26842	CD27 antigen	199.16	2.759
Q5ZPR3	CD276 antigen	235.14	2.728
Q8IX05	CD302 antigen	237.65	2.629
Q9NPF0	CD320 antigen	197.90	2.498
P16070	CD44 antigen	262.76	2.428
Q01151	CD83 antigen	238.91	2.628
P14209	CD99 antigen	210.87	2.473
Q8TCZ2	CD99 antigen-like protein 2	154.81	2.915
Q9BY67	Cell adhesion molecule 1	274.89	2.579
Q8N3J6	Cell adhesion molecule 2	247.27	2.721
Q8N126	Cell adhesion molecule 3	282.42	2.308
Q8NFZ8	Cell adhesion molecule 4	275.31	2.533
Q99795	Cell surface A33 antigen	253.55	2.373
Q8TD46	Cell surface glycoprotein CD200 rec...	214.64	2.532
Q6Q8B3	Cell surface glycoprotein CD200 rec...	210.46	2.630
P43121	Cell surface glycoprotein MUC18	308.78	2.488
Q6UVK1	Chondroitin sulfate proteoglycan 4	253.55	2.471
O95196	Chondroitin sulfate proteoglycan 5	223.01	2.476
Q9H9P2	Chondrolectin	216.31	2.710
Q8TDQ1	CMRF35-like molecule 1	253.13	2.247
Q496F6	CMRF35-like molecule 2	202.92	2.486
Q6UXZ3	CMRF35-like molecule 4	186.61	2.304
Q08708	CMRF35-like molecule 6	207.11	2.339
A8K4G0	CMRF35-like molecule 7	235.56	2.703
Q9UGN4	CMRF35-like molecule 8	234.72	1.780
Q6UXG3	CMRF35-like molecule 9	221.33	2.644
Q9HBJ8	Collectrin	298.74	2.204
Q9NPY3	Complement component C1q receptor	256.06	2.247
P17927	Complement receptor type 1	267.78	2.551
P20023	Complement receptor type 2	274.89	3.017
P78357	Contactin-associated protein 1	260.24	2.074
Q9UHC6	Contactin-associated protein-like 2	263.17	2.535

Q9BZ76	Contactin-associated protein-like 3	272.38	2.512
Q96NU0	Contactin-associated protein-like 3...	261.50	2.710
Q9C0A0	Contactin-associated protein-like 4	269.45	2.579
Q8WYK1	Contactin-associated protein-like 5	272.80	2.226
P78310	Coxsackievirus and adenovirus recep...	242.25	2.162
Q86T13	C-type lectin domain family 14 memb...	252.71	2.380
Q9UBG0	C-type mannose receptor 2	283.26	2.049
Q96PZ7	CUB and sushi domain-containing pro...	203.76	2.569
Q86UP6	CUB and zona pellucida-like domain...	178.24	2.785
Q9H6B4	CXADR-like membrane protein	227.19	2.602
Q9H2A7	C-X-C motif chemokine 16	230.96	2.828
Q96J86	Cysteine and tyrosine-rich protein ...	239.32	2.147
Q9NZV1	Cysteine-rich motor neuron 1 protei...	270.70	2.416
P32927	Cytokine receptor common subunit be...	235.98	2.168
P31785	Cytokine receptor common subunit ga...	197.90	2.936
Q9HC73	Cytokine receptor-like factor 2	227.19	2.280
O95727	Cytotoxic and regulatory T-cell mol...	266.52	2.109
P16410	Cytotoxic T-lymphocyte protein 4	169.87	2.633
Q8NFT8	Delta and Notch-like epidermal grow...	291.21	2.437
O00548	Delta-like protein 1	287.44	2.523
Q9NYJ7	Delta-like protein 3	190.79	2.170
Q9NR61	Delta-like protein 4	240.58	2.265
Q08554	Desmocollin-1	251.88	2.961
Q02487	Desmocollin-2	252.30	2.528
Q14574	Desmocollin-3	241.42	2.555
Q02413	Desmoglein-1	220.50	2.535
Q14126	Desmoglein-2	288.70	2.233
P32926	Desmoglein-3	258.57	1.839
Q86SJ6	Desmoglein-4	244.76	2.262
Q3MIW9	Diffuse panbronchiolitis critical r...	321.33	2.016
Q8N8Z6	Discoidin, CUB and LCCL domain-cont...	234.72	2.552
Q96PD2	Discoidin, CUB and LCCL domain-cont...	264.85	2.432
Q16832	Discoidin domain-containing recepto...	315.89	2.311
O14672	Disintegrin and metalloproteinase d...	182.84	2.856
O75078	Disintegrin and metalloproteinase d...	194.14	2.584
O43184	Disintegrin and metalloproteinase d...	227.19	2.769
Q13444	Disintegrin and metalloproteinase d...	186.61	2.522
P78536	Disintegrin and metalloproteinase d...	192.88	2.671
Q9Y3Q7	Disintegrin and metalloproteinase d...	215.06	2.421
Q9H013	Disintegrin and metalloproteinase d...	249.78	2.487
Q99965	Disintegrin and metalloproteinase d...	240.16	2.454
O43506	Disintegrin and metalloproteinase d...	234.30	2.113
Q9UKJ8	Disintegrin and metalloproteinase d...	194.97	2.571
Q9P0K1	Disintegrin and metalloproteinase d...	243.51	2.320
O75077	Disintegrin and metalloproteinase d...	192.46	2.584
Q9UKQ2	Disintegrin and metalloproteinase d...	255.64	2.512

Q9UKF5	Disintegrin and metalloproteinase d...	239.32	2.226
Q9UKF2	Disintegrin and metalloproteinase d...	256.06	2.283
Q8TC27	Disintegrin and metalloproteinase d...	222.17	2.710
Q9BZ11	Disintegrin and metalloproteinase d...	179.08	2.471
Q9H2U9	Disintegrin and metalloproteinase d...	306.27	2.070
P78325	Disintegrin and metalloproteinase d...	297.48	2.144
Q13443	Disintegrin and metalloproteinase d...	278.65	2.335
O60469	Down syndrome cell adhesion molecul...	284.51	2.269
Q8TD84	Down syndrome cell adhesion molecul...	221.75	2.780
Q5VV43	Dyslexia-associated protein KIAA031...	172.38	2.707
Q14118	Dystroglycan	251.46	3.090
Q86XS8	E3 ubiquitin-protein ligase RNF130	234.30	2.603
Q68DV7	E3 ubiquitin-protein ligase RNF43	208.78	2.991
Q9ULT6	E3 ubiquitin-protein ligase ZNRF3	255.64	2.553
Q6PCB8	Embigin	218.82	2.805
Q902F9	Endogenous retrovirus group K membe...	230.12	2.567
O71037	Endogenous retrovirus group K membe...	230.12	2.567
P61565	Endogenous retrovirus group K membe...	230.12	2.567
Q69384	Endogenous retrovirus group K membe...	230.12	2.567
Q902F8	Endogenous retrovirus group K membe...	230.12	2.567
Q9UKH3	Endogenous retrovirus group K membe...	230.12	2.567
Q9H9K5	Endogenous retrovirus group MER34 m...	232.21	2.630
B6SEH8	Endogenous retrovirus group V membe...	141.42	2.579
P17813	Endoglin	223.84	2.679
Q9ULC0	Endomucin	267.78	2.574
Q9HCU0	Endosialin	261.50	2.477
Q96AP7	Endothelial cell-selective adhesion...	212.13	2.136
Q19T08	Endothelial cell-specific chemotaxi...	300.83	1.969
Q9UNN8	Endothelial protein C receptor	236.40	2.435
P21709	Ephrin type-A receptor 1	261.50	2.230
Q5JZY3	Ephrin type-A receptor 10	222.17	2.659
P29317	Ephrin type-A receptor 2	236.81	2.208
P29320	Ephrin type-A receptor 3	290.79	2.761
P54764	Ephrin type-A receptor 4	275.73	2.340
P54756	Ephrin type-A receptor 5	266.10	2.452
Q9UF33	Ephrin type-A receptor 6	216.73	2.463
Q15375	Ephrin type-A receptor 7	257.32	2.458
P29322	Ephrin type-A receptor 8	264.85	2.452
P54762	Ephrin type-B receptor 1	240.16	2.620
P29323	Ephrin type-B receptor 2	245.60	2.474
P54753	Ephrin type-B receptor 3	245.18	2.401
P54760	Ephrin type-B receptor 4	277.40	2.167
O15197	Ephrin type-B receptor 6	235.14	2.512
P98172	Ephrin-B1	264.01	2.421
P52799	Ephrin-B2	268.19	2.608
Q15768	Ephrin-B3	155.64	1.873

P00533	Epidermal growth factor receptor	242.25	2.596
Q6UW88	Epigen	194.56	2.738
P16422	Epithelial cell adhesion molecule	330.12	1.930
Q08345	Epithelial discoidin domain-contain...	305.43	2.200
Q8N766	ER membrane protein complex subunit...	122.59	3.142
Q5UCC4	ER membrane protein complex subunit...	135.98	3.183
Q9NPA0	ER membrane protein complex subunit...	195.39	2.327
Q96PL5	Erythroid membrane-associated prote...	292.88	2.487
P19235	Erythropoietin receptor	296.65	2.141
P16581	E-selectin	179.08	2.476
Q86XX4	Extracellular matrix protein FRAS1	253.97	2.630
Q96LA6	Fc receptor-like protein 1	129.70	3.181
Q96LA5	Fc receptor-like protein 2	177.82	2.378
Q96P31	Fc receptor-like protein 3	211.29	2.432
Q96PJ5	Fc receptor-like protein 4	192.05	2.250
Q96RD9	Fc receptor-like protein 5	160.67	2.720
Q6DN72	Fc receptor-like protein 6	198.74	2.754
P11362	Fibroblast growth factor receptor 1	187.02	3.086
P21802	Fibroblast growth factor receptor 2	252.30	2.895
P22607	Fibroblast growth factor receptor 3	217.15	2.838
P22455	Fibroblast growth factor receptor 4	191.63	2.488
Q8N441	Fibroblast growth factor receptor-l...	207.53	2.919
P08F94	Fibrocystin	182.84	2.620
F2Z333	Fibronectin type III domain-contain...	235.98	2.951
Q9H6D8	Fibronectin type III domain-contain...	233.05	2.864
Q8NAU1	Fibronectin type III domain-contain...	227.19	2.875
P49771	Fms-related tyrosine kinase 3 ligan...	222.59	2.022
P78423	Fractalkine	193.30	2.599
Q5SZK8	FRAS1-related extracellular matrix ...	198.32	2.756
P09958	Furin	259.41	2.603
Q14802	FXFD domain-containing ion transpor...	209.20	2.892
P59646	FXFD domain-containing ion transpor...	179.08	2.584
Q96DB9	FXFD domain-containing ion transpor...	186.61	2.684
Q9H0Q3	FXFD domain-containing ion transpor...	219.66	2.700
P02724	Glycophorin-A	220.50	2.803
P06028	Glycophorin-B	279.91	2.698
P15421	Glycophorin-E	206.69	2.895
Q9NU53	Glycoprotein integral membrane prot...	193.30	2.852
P55808	Glycoprotein Xg	182.42	2.864
Q92896	Golgi apparatus protein 1	195.39	2.764
I3L273	Golgi-associated olfactory signalin...	227.61	2.569
Q99062	Granulocyte colony-stimulating fact...	227.19	2.417
P15509	Granulocyte-macrophage colony-stimu...	235.14	2.814
P10912	Growth hormone receptor	248.11	2.606
P25092	Heat-stable enterotoxin receptor	293.72	2.481
Q9UBK5	Hematopoietic cell signal transduce...	204.18	2.479

P28906	Hematopoietic progenitor cell antig...	182.84	2.769
Q96D42	Hepatitis A virus cellular receptor...	246.02	2.756
Q8TDQ0	Hepatitis A virus cellular receptor...	205.43	2.379
Q14CZ8	Hepatocyte cell adhesion molecule	197.48	2.919
P08581	Hepatocyte growth factor receptor	220.08	2.624
Q9BQS7	Hephaestin	238.91	2.527
Q6MZM0	Hephaestin-like protein 1	264.85	2.360
Q30201	Hereditary hemochromatosis protein	284.09	2.395
Q8WWV6	High affinity immunoglobulin alpha ...	174.05	2.667
P12319	High affinity immunoglobulin epsilo...	201.25	2.575
P30273	High affinity immunoglobulin epsilo...	189.95	2.762
P12314	High affinity immunoglobulin gamma ...	196.65	2.947
Q92637	High affinity immunoglobulin gamma ...	196.65	2.947
P04629	High affinity nerve growth factor r...	189.12	2.135
P30443	HLA class I histocompatibility anti...	241.84	2.725
P13746	HLA class I histocompatibility anti...	241.84	2.725
P01892	HLA class I histocompatibility anti...	237.65	2.707
P30447	HLA class I histocompatibility anti...	241.84	2.725
P05534	HLA class I histocompatibility anti...	241.84	2.725
P18462	HLA class I histocompatibility anti...	248.11	2.544
P30450	HLA class I histocompatibility anti...	248.11	2.544
P30512	HLA class I histocompatibility anti...	214.22	2.500
P04439	HLA class I histocompatibility anti...	241.84	2.725
P16188	HLA class I histocompatibility anti...	241.84	2.725
P16189	HLA class I histocompatibility anti...	214.22	2.500
P10314	HLA class I histocompatibility anti...	204.60	2.663
P16190	HLA class I histocompatibility anti...	214.22	2.500
P30453	HLA class I histocompatibility anti...	245.18	2.544
P30455	HLA class I histocompatibility anti...	241.84	2.725
P30456	HLA class I histocompatibility anti...	248.11	2.544
P30457	HLA class I histocompatibility anti...	248.11	2.544
P01891	HLA class I histocompatibility anti...	237.65	2.707
P10316	HLA class I histocompatibility anti...	227.19	2.455
P30459	HLA class I histocompatibility anti...	204.60	2.663
Q09160	HLA class I histocompatibility anti...	252.30	2.563
P13747	HLA class I histocompatibility anti...	240.16	2.620
P30511	HLA class I histocompatibility anti...	241.00	2.496
P17693	HLA class I histocompatibility anti...	238.49	2.551
P30461	HLA class I histocompatibility anti...	249.78	2.574
P30462	HLA class I histocompatibility anti...	249.78	2.574
P30464	HLA class I histocompatibility anti...	239.32	2.736
P30466	HLA class I histocompatibility anti...	239.32	2.736
P03989	HLA class I histocompatibility anti...	286.19	2.385
P30685	HLA class I histocompatibility anti...	275.73	2.548
P18463	HLA class I histocompatibility anti...	275.73	2.548
Q95365	HLA class I histocompatibility anti...	286.19	2.385

P30475	HLA class I histocompatibility anti...	286.19	2.385
Q04826	HLA class I histocompatibility anti...	286.19	2.385
P30479	HLA class I histocompatibility anti...	249.78	2.574
P30480	HLA class I histocompatibility anti...	249.78	2.574
P30481	HLA class I histocompatibility anti...	249.78	2.574
P30483	HLA class I histocompatibility anti...	239.32	2.736
P30484	HLA class I histocompatibility anti...	239.32	2.736
P30485	HLA class I histocompatibility anti...	259.41	2.385
P30486	HLA class I histocompatibility anti...	249.78	2.574
P30487	HLA class I histocompatibility anti...	239.32	2.736
P30488	HLA class I histocompatibility anti...	239.32	2.736
P18464	HLA class I histocompatibility anti...	275.73	2.548
P30490	HLA class I histocompatibility anti...	275.73	2.548
P30491	HLA class I histocompatibility anti...	275.73	2.548
P30492	HLA class I histocompatibility anti...	275.73	2.548
P30493	HLA class I histocompatibility anti...	275.73	2.548
P30495	HLA class I histocompatibility anti...	275.73	2.548
P18465	HLA class I histocompatibility anti...	286.19	2.385
P10319	HLA class I histocompatibility anti...	275.73	2.548
Q29940	HLA class I histocompatibility anti...	275.73	2.548
Q29836	HLA class I histocompatibility anti...	286.19	2.385
P01889	HLA class I histocompatibility anti...	249.78	2.574
Q31612	HLA class I histocompatibility anti...	301.25	2.341
P30498	HLA class I histocompatibility anti...	275.73	2.548
P30460	HLA class I histocompatibility anti...	249.78	2.574
Q31610	HLA class I histocompatibility anti...	286.19	2.385
Q29718	HLA class I histocompatibility anti...	275.73	2.548
P30499	HLA class I histocompatibility anti...	299.16	2.372
P30508	HLA class I histocompatibility anti...	289.53	2.473
P30510	HLA class I histocompatibility anti...	299.16	2.372
Q07000	HLA class I histocompatibility anti...	289.53	2.473
Q29960	HLA class I histocompatibility anti...	299.16	2.372
Q95604	HLA class I histocompatibility anti...	272.38	1.968
Q29865	HLA class I histocompatibility anti...	309.20	2.341
P30501	HLA class I histocompatibility anti...	299.16	2.372
P04222	HLA class I histocompatibility anti...	299.16	2.372
P30504	HLA class I histocompatibility anti...	289.53	2.473
Q9TNN7	HLA class I histocompatibility anti...	289.53	2.473
Q29963	HLA class I histocompatibility anti...	289.53	2.473
P10321	HLA class I histocompatibility anti...	269.45	2.693
P30505	HLA class I histocompatibility anti...	289.53	2.473
P06340	HLA class II histocompatibility ant...	246.86	2.635
P13765	HLA class II histocompatibility ant...	243.93	2.535
P20036	HLA class II histocompatibility ant...	264.01	2.562
P04440	HLA class II histocompatibility ant...	172.80	2.689
P01909	HLA class II histocompatibility ant...	241.00	2.683

P01906	HLA class II histocompatibility ant...	229.70	2.892
P01920	HLA class II histocompatibility ant...	206.27	2.213
P05538	HLA class II histocompatibility ant...	206.27	2.213
P01903	HLA class II histocompatibility ant...	233.47	2.722
P79483	HLA class II histocompatibility ant...	192.88	2.433
P13762	HLA class II histocompatibility ant...	192.88	2.433
Q30154	HLA class II histocompatibility ant...	186.61	2.313
P04229	HLA class II histocompatibility ant...	192.88	2.433
Q30167	HLA class II histocompatibility ant...	192.88	2.433
P20039	HLA class II histocompatibility ant...	192.88	2.433
P01911	HLA class II histocompatibility ant...	186.61	2.313
P01912	HLA class II histocompatibility ant...	192.88	2.433
P13760	HLA class II histocompatibility ant...	192.88	2.433
P13761	HLA class II histocompatibility ant...	192.88	2.433
Q30134	HLA class II histocompatibility ant...	192.88	2.433
Q9TQE0	HLA class II histocompatibility ant...	192.88	2.433
O75144	ICOS ligand	237.65	2.761
Q9H665	IGF-like family receptor 1	309.62	1.962
P55899	IgG receptor FcRn large subunit p51	255.22	2.542
A6NFU0	Ig-like V-type domain-containing pr...	167.36	2.916
P24071	Immunoglobulin alpha Fc receptor	220.92	2.484
Q8IVU1	Immunoglobulin superfamily DCC subc...	249.78	2.504
Q8TDY8	Immunoglobulin superfamily DCC subc...	226.35	2.606
Q5DX21	Immunoglobulin superfamily member 1...	241.42	2.477
Q93033	Immunoglobulin superfamily member 2	260.24	1.978
O75054	Immunoglobulin superfamily member 3	200.83	2.323
Q9NSI5	Immunoglobulin superfamily member 5	115.48	2.776
O95976	Immunoglobulin superfamily member 6	199.58	2.852
Q86SU0	Immunoglobulin-like domain-containi...	257.32	2.532
Q13308	Inactive tyrosine-protein kinase 7	187.44	2.864
Q01973	Inactive tyrosine-protein kinase tr...	243.09	2.576
Q9Y6W8	Inducible T-cell costimulator	231.79	2.821
Q6GPH6	Inositol 1,4,5-trisphosphate recept...	115.06	2.730
Q3MIP1	Inositol 1,4,5-trisphosphate recept...	166.94	2.627
P06213	Insulin receptor	253.97	2.466
P14616	Insulin receptor-related protein Insulin-	210.04	2.516
P08069	like growth factor 1 recept... Integral	264.43	2.821
P98153	membrane protein DGCR2/IDD Integrin	214.22	2.311
P56199	alpha-1	259.83	2.351
O75578	Integrin alpha-10	245.60	2.474
Q9UKX5	Integrin alpha-11	230.96	2.609
P17301	Integrin alpha-2	253.97	2.526
P26006	Integrin alpha-3	267.78	2.195
P13612	Integrin alpha-4	225.52	2.751
P08648	Integrin alpha-5	282.42	2.440
P23229	Integrin alpha-6	279.07	2.746

Q13683	Integrin alpha-7	281.16	1.973
P53708	Integrin alpha-8	267.78	2.331
Q13797	Integrin alpha-9	274.47	2.360
Q13349	Integrin alpha-D	190.79	2.887
P38570	Integrin alpha-E	258.99	2.483
P08514	Integrin alpha-IIb	251.04	2.844
P20701	Integrin alpha-L	227.19	2.244
P11215	Integrin alpha-M	189.12	2.855
P06756	Integrin alpha-V	279.07	2.705
P20702	Integrin alpha-X	197.90	2.718
P05556	Integrin beta-1	269.87	2.583
P05107	Integrin beta-2	256.06	2.599
P05106	Integrin beta-3	275.31	2.632
P16144	Integrin beta-4	246.44	1.775
P18084	Integrin beta-5	245.18	2.821
P18564	Integrin beta-6	245.18	2.821
P26010	Integrin beta-7	190.79	2.873
P26012	Integrin beta-8	256.48	2.115
P05362	Intercellular adhesion molecule 1	189.12	3.012
P13598	Intercellular adhesion molecule 2	296.65	2.486
P32942	Intercellular adhesion molecule 3	277.40	2.613
Q14773	Intercellular adhesion molecule 4	169.87	2.774
Q9UMF0	Intercellular adhesion molecule 5	145.18	2.035
P17181	Interferon alpha/beta receptor 1	223.43	2.816
P48551	Interferon alpha/beta receptor 2	211.29	2.610
P15260	Interferon gamma receptor 1	240.58	2.469
P38484	Interferon gamma receptor 2	198.32	2.766
Q8IU57	Interferon lambda receptor 1	230.12	2.667
Q9NPH3	Interleukin-1 receptor accessory pr...	217.15	2.567
Q9NZN1	Interleukin-1 receptor accessory pr...	199.16	2.813
P14778	Interleukin-1 receptor type 1	191.21	2.990
P27930	Interleukin-1 receptor type 2	170.71	3.074
Q01638	Interleukin-1 receptor-like 1	255.64	2.805
Q9HB29	Interleukin-1 receptor-like 2	199.16	2.684
Q13651	Interleukin-10 receptor subunit alp...	233.47	2.576
Q08334	Interleukin-10 receptor subunit bet...	234.72	2.898
Q14626	Interleukin-11 receptor subunit alp...	180.75	2.401
P42701	Interleukin-12 receptor subunit bet...	216.73	2.567
Q99665	Interleukin-12 receptor subunit bet...	179.91	3.006
P78552	Interleukin-13 receptor subunit alp...	276.56	2.782
Q14627	Interleukin-13 receptor subunit alp...	217.15	2.384
Q13261	Interleukin-15 receptor subunit alp...	184.10	2.914
Q96F46	Interleukin-17 receptor A	217.57	2.741
Q9NRM6	Interleukin-17 receptor B	200.83	2.833
Q8NAC3	Interleukin-17 receptor C	228.45	2.240
Q8NFM7	Interleukin-17 receptor D	200.00	2.721

Q8NFR9	Interleukin-17 receptor E	261.08	1.927
Q13478	Interleukin-18 receptor 1	285.35	2.659
O95256	Interleukin-18 receptor accessory p...	209.62	2.629
P01589	Interleukin-2 receptor subunit alph...	211.71	2.539
P14784	Interleukin-2 receptor subunit beta	213.38	2.854
Q9UHF4	Interleukin-20 receptor subunit alp...	169.03	2.992
Q6UXL0	Interleukin-20 receptor subunit bet...	265.27	2.306
Q9HBE5	Interleukin-21 receptor	164.43	2.755
Q8N6P7	Interleukin-22 receptor subunit alp...	154.81	2.705
Q5VWK5	Interleukin-23 receptor	242.67	2.571
Q6UWB1	Interleukin-27 receptor subunit alp...	184.51	2.547
P26951	Interleukin-3 receptor subunit alph...	222.59	2.758
Q8NI17	Interleukin-31 receptor subunit alp...	238.07	2.396
P24394	Interleukin-4 receptor subunit alph...	258.57	2.861
Q01344	Interleukin-5 receptor subunit alph...	265.27	2.614
P08887	Interleukin-6 receptor subunit alph...	194.56	2.780
P40189	Interleukin-6 receptor subunit beta	241.42	2.628
P16871	Interleukin-7 receptor subunit alph...	264.85	2.794
Q01113	Interleukin-9 receptor	138.07	2.916
Q9BZV3	Interphotoreceptor matrix proteogly...	247.69	2.548
Q8IYV9	Izumo sperm-egg fusion protein 1	202.51	2.492
Q6UXV1	Izumo sperm-egg fusion protein 2	273.22	2.338
Q5VZ72	Izumo sperm-egg fusion protein 3	248.53	2.433
Q9Y624	Junctional adhesion molecule A	253.55	2.566
P57087	Junctional adhesion molecule B	246.44	2.587
Q9BX67	Junctional adhesion molecule C	228.86	2.429
Q86YT9	Junctional adhesion molecule-like	287.02	2.548
Q8NC54	Keratinocyte-associated transmembra...	166.52	2.733
P43626	Killer cell immunoglobulin-like rec...	251.88	2.171
P43627	Killer cell immunoglobulin-like rec...	251.88	2.171
P43628	Killer cell immunoglobulin-like rec...	266.52	2.177
Q99706	Killer cell immunoglobulin-like rec...	173.64	2.933
Q8N109	Killer cell immunoglobulin-like rec...	243.09	2.401
Q8NHK3	Killer cell immunoglobulin-like rec...	243.09	2.401
Q14954	Killer cell immunoglobulin-like rec...	174.05	2.677
P43631	Killer cell immunoglobulin-like rec...	189.95	2.641
Q14952	Killer cell immunoglobulin-like rec...	171.13	2.632
P43632	Killer cell immunoglobulin-like rec...	189.95	2.641
Q14953	Killer cell immunoglobulin-like rec...	171.13	2.632
P43629	Killer cell immunoglobulin-like rec...	267.78	2.134
P43630	Killer cell immunoglobulin-like rec...	259.41	2.139
Q8N743	Killer cell immunoglobulin-like rec...	222.17	2.725
Q14943	Killer cell immunoglobulin-like rec...	191.21	2.617
Q96J84	Kin of IRRE-like protein 1	228.03	2.411
Q6UWL6	Kin of IRRE-like protein 2	186.19	2.661
Q8IZU9	Kin of IRRE-like protein 3	235.56	2.579

P21583	Kit ligand	163.18	2.766
Q9UEF7	Klotho	220.50	2.108
Q96MU8	Kremen protein 1	194.97	2.748
Q8NCW0	Kremen protein 2	208.36	2.647
O43291	Kunitz-type protease inhibitor 2	251.46	2.494
P09848	Lactase-phlorizin hydrolase	200.83	2.409
Q6UX15	Layilin	223.84	2.684
P48357	Leptin receptor	221.33	2.844
Q9P244	Leucine-rich repeat and fibronectin...	276.56	2.538
Q9ULH4	Leucine-rich repeat and fibronectin...	285.35	2.479
Q9BTN0	Leucine-rich repeat and fibronectin...	266.52	2.566
Q6PJG9	Leucine-rich repeat and fibronectin...	235.14	2.186
Q96NI6	Leucine-rich repeat and fibronectin...	293.30	2.247
Q96FE5	Leucine-rich repeat and immunoglobu...	218.82	2.633
Q7L985	Leucine-rich repeat and immunoglobu...	217.15	2.525
P0C6S8	Leucine-rich repeat and immunoglobu...	225.94	2.740
Q6UY18	Leucine-rich repeat and immunoglobu...	192.88	2.916
Q9HBL6	Leucine-rich repeat and transmembra...	225.10	3.023
Q8N967	Leucine-rich repeat and transmembra...	237.65	2.563
Q6UXK5	Leucine-rich repeat neuronal protei...	182.00	2.780
O75325	Leucine-rich repeat neuronal protei...	218.40	2.123
Q9H3W5	Leucine-rich repeat neuronal protei...	225.10	2.665
Q8WUT4	Leucine-rich repeat neuronal protei...	182.42	2.512
Q86UE6	Leucine-rich repeat transmembrane n...	229.28	2.761
O43300	Leucine-rich repeat transmembrane n...	235.98	2.454
Q86VH5	Leucine-rich repeat transmembrane n...	255.64	2.569
Q86VH4	Leucine-rich repeat transmembrane n...	237.65	2.782
Q8TF66	Leucine-rich repeat-containing prot...	244.35	2.527
Q9H756	Leucine-rich repeat-containing prot...	232.63	2.589
Q8N386	Leucine-rich repeat-containing prot...	203.76	2.756
Q2I0M4	Leucine-rich repeat-containing prot...	157.74	2.859
Q14392	Leucine-rich repeat-containing prot...	239.74	2.502
A6NMS7	Leucine-rich repeat-containing prot...	284.51	2.381
A6NM11	Leucine-rich repeat-containing prot...	284.51	2.381
O60309	Leucine-rich repeat-containing prot...	287.02	2.218
Q96QE4	Leucine-rich repeat-containing prot...	303.34	2.237
Q9HBW1	Leucine-rich repeat-containing prot...	237.65	2.857
Q96JA1	Leucine-rich repeats and immunoglob...	223.84	2.724
O94898	Leucine-rich repeats and immunoglob...	278.65	2.416
P42702	Leukemia inhibitory factor receptor	300.41	2.777
O75019	Leukocyte immunoglobulin-like recep...	200.83	2.733
Q8N149	Leukocyte immunoglobulin-like recep...	199.58	2.710
P59901	Leukocyte immunoglobulin-like recep...	192.05	2.623
A6NI73	Leukocyte immunoglobulin-like recep...	135.56	3.222
Q6PI73	Leukocyte immunoglobulin-like recep...	184.10	2.725
Q8NHL6	Leukocyte immunoglobulin-like recep...	320.49	1.827

Q8N423	Leukocyte immunoglobulin-like recep...	319.24	1.827
O75022	Leukocyte immunoglobulin-like recep...	285.77	1.923
Q8NHJ6	Leukocyte immunoglobulin-like recep...	286.19	1.863
O75023	Leukocyte immunoglobulin-like recep...	265.68	1.974
P29376	Leukocyte tyrosine kinase receptor	280.33	2.752
Q6GTX8	Leukocyte-associated immunoglobulin...	286.19	2.171
P16150	Leukosialin	297.06	2.261
Q86UK5	Limbin	215.06	2.633
P12318	Low affinity immunoglobulin gamma F...	284.93	2.121
P31994	Low affinity immunoglobulin gamma F...	193.30	2.703
P31995	Low affinity immunoglobulin gamma F...	275.73	2.310
P08637	Low affinity immunoglobulin gamma F...	181.17	2.857
P01130	Low-density lipoprotein receptor	261.08	2.603
Q5SZI1	Low-density lipoprotein receptor cl...	63.18	2.822
Q86YD5	Low-density lipoprotein receptor cl...	244.35	2.592
Q7Z4F1	Low-density lipoprotein receptor-re...	228.03	2.779
Q86VZ4	Low-density lipoprotein receptor-re...	223.01	2.691
Q9Y561	Low-density lipoprotein receptor-re...	229.28	2.779
Q9NZR2	Low-density lipoprotein receptor-re...	275.31	2.610
P98164	Low-density lipoprotein receptor-re...	279.91	2.430
O75074	Low-density lipoprotein receptor-re...	226.35	2.748
O75096	Low-density lipoprotein receptor-re...	240.16	2.659
O75197	Low-density lipoprotein receptor-re...	201.25	3.005
O75581	Low-density lipoprotein receptor-re...	160.67	2.559
Q14114	Low-density lipoprotein receptor-re...	238.07	2.951
Q8ND94	LRRN4 C-terminal-like protein	182.42	2.625
P14151	L-selectin	205.02	2.994
Q9Y5Y7	Lymphatic vessel endothelial hyalur...	203.34	2.273
P18627	Lymphocyte activation gene 3 protei...	228.45	2.205
Q5SQ64	Lymphocyte antigen 6 complex locus ...	219.66	2.813
O60449	Lymphocyte antigen 75	241.00	3.001
P19256	Lymphocyte function-associated anti...	179.91	3.236
Q9UJQ1	Lysosome-associated membrane glycop...	215.89	2.790
P07333	Macrophage colony-stimulating facto...	263.17	2.394
P22897	Macrophage mannose receptor 1	224.26	2.630
Q2M385	Macrophage-expressed gene 1 protein	198.74	2.489
Q04912	Macrophage-stimulating protein rece...	243.51	2.188
P34810	Macrosialin	335.56	2.239
Q95460	Major histocompatibility complex cl...	191.63	2.718
Q9H8J5	MANSC domain-containing protein 1	246.86	2.221
A6NHS7	MANSC domain-containing protein 4	225.94	2.936
P10721	Mast/stem cell growth factor recept...	236.40	2.919
P50281	Matrix metalloproteinase-14	274.47	1.909
P51511	Matrix metalloproteinase-15	240.16	2.481
P51512	Matrix metalloproteinase-16	257.73	2.741
Q9Y5R2	Matrix metalloproteinase-24	248.53	2.836

Q9BRK3	Matrix-remodeling-associated protei...	244.35	2.247
P15529	Membrane cofactor protein	285.35	2.368
Q8TBP5	Membrane protein FAM174A	187.86	2.686
Q3ZCQ3	Membrane protein FAM174B	217.57	2.494
Q16819	Meprin A subunit alpha	209.62	3.047
Q16820	Meprin A subunit beta	240.58	2.669
Q96KJ4	Mesothelin-like protein	203.34	3.280
Q86V40	Metalloprotease TIKI1	163.18	2.761
A6NFA1	Metalloprotease TIKI2	162.76	2.995
Q29983	MHC class I polypeptide-related seq...	178.66	2.571
Q29980	MHC class I polypeptide-related seq...	192.88	2.916
P55082	Microfibril-associated glycoprotein...	172.80	3.190
O75121	Microfibrillar-associated protein 3...	184.51	3.157
P15941	Mucin-1	285.35	2.610
Q9UKN1	Mucin-12	281.16	2.407
Q9H3R2	Mucin-13	243.93	2.642
Q8N387	Mucin-15	200.83	2.592
Q8WXI7	Mucin-16	225.94	2.800
Q5SSG8	Mucin-21	231.38	2.514
Q13477	Mucosal addressin cell adhesion mol...	143.51	2.583
Q96KG7	Multiple epidermal growth factor-li...	305.43	2.141
A6BM72	Multiple epidermal growth factor-li...	250.20	2.433
Q7Z7M0	Multiple epidermal growth factor-li...	236.81	1.778
Q9H1U4	Multiple epidermal growth factor-li...	287.02	2.447
O15146	Muscle, skeletal receptor tyrosine-...	191.63	2.744
P25189	Myelin protein P0	286.60	2.204
O95297	Myelin protein zero-like protein 1	223.84	2.644
O60487	Myelin protein zero-like protein 2	267.36	2.705
Q6UWV2	Myelin protein zero-like protein 3	258.15	2.250
P20916	Myelin-associated glycoprotein	186.19	2.871
P20138	Myeloid cell surface antigen CD33	235.98	2.641
O76036	Natural cytotoxicity triggering rec...	170.29	2.761
O95944	Natural cytotoxicity triggering rec...	205.02	2.567
O14931	Natural cytotoxicity triggering rec...	150.21	2.738
Q68D85	Natural cytotoxicity triggering rec...	181.17	2.800
Q9BZW8	Natural killer cell receptor 2B4	251.88	2.689
Q15223	Nectin-1	243.09	2.322
Q92692	Nectin-2	218.40	2.189
Q96NY8	Nectin-4	309.62	2.016
Q86YC3	Negative regulator of reactive oxyg...	226.35	2.790
Q92859	Neogenin	298.32	2.149
O60500	Nephrin	146.44	2.185
P43146	Netrin receptor DCC	342.67	2.277
Q6ZN44	Netrin receptor UNC5A	288.70	2.320
Q8IZJ1	Netrin receptor UNC5B	274.05	2.221
O95185	Netrin receptor UNC5C	287.44	2.401

Q6UXZ4	Netrin receptor UNC5D	214.64	2.553
P13591	Neural cell adhesion molecule 1	269.87	2.479
O15394	Neural cell adhesion molecule 2	233.47	2.201
P32004	Neural cell adhesion molecule L1	283.26	2.516
O00533	Neural cell adhesion molecule L1-li...	243.93	2.659
Q9ULB1	Neurexin-1	228.03	2.815
P58400	Neurexin-1-beta	210.87	3.084
Q9P2S2	Neurexin-2	228.03	2.815
P58401	Neurexin-2-beta	228.03	2.815
Q9Y4C0	Neurexin-3	228.03	2.815
Q9HDB5	Neurexin-3-beta	228.03	2.815
O94856	Neurofascin	290.37	2.494
P46531	Neurogenic locus notch homolog prot...	220.50	2.455
Q04721	Neurogenic locus notch homolog prot...	295.39	2.281
Q9UM47	Neurogenic locus notch homolog prot...	264.43	2.320
Q99466	Neurogenic locus notch homolog prot...	213.38	2.659
Q8N2Q7	Neuroigin-1	185.35	2.775
Q8NFZ4	Neuroigin-2	184.10	2.739
Q9NZ94	Neuroigin-3	184.10	2.739
Q8N0W4	Neuroigin-4, X-linked	185.35	2.775
Q8NFZ3	Neuroigin-4, Y-linked	185.35	2.775
Q92823	Neuronal cell adhesion molecule	284.93	2.696
Q8TDF5	Neuropilin and tolloid-like protein...	257.73	2.386
Q8NC67	Neuropilin and tolloid-like protein...	230.54	2.432
O14786	Neuropilin-1	254.81	2.910
O60462	Neuropilin-2	222.17	2.997
Q9Y639	Neuroplastin	233.89	2.746
Q8NET5	NFAT activation molecule 1	193.30	2.285
Q92542	Nicastrin	205.85	2.721
Q8TD07	NKG2D ligand 4	230.54	2.876
Q15155	Nodal modulator 1	116.73	3.142
P69849	Nodal modulator 3	116.73	3.142
Q5T1S8	Noncompact myelin-associated protei...	313.80	2.098
Q16288	NT-3 growth factor receptor	283.68	2.645
Q99650	Oncostatin-M-specific receptor subu...	235.56	2.733
Q96PE5	Opalin	217.57	2.360
P41217	OX-2 membrane glycoprotein	261.92	2.538
Q9UKJ1	Paired immunoglobulin-like type 2 r...	249.37	2.739
Q9UKJ0	Paired immunoglobulin-like type 2 r...	244.35	2.426
Q9UMZ3	Phosphatidylinositol phosphatase PT...	233.05	2.669
Q96FE7	Phosphoinositide-3-kinase-interacti...	214.64	2.695
O00168	Phospholemman	241.42	2.293
Q6P1J6	Phospholipase B1, membrane-associat...	175.31	2.659
Q8IYJ0	PILR alpha-associated neural protei...	201.67	2.762
P53801	Pituitary tumor-transforming gene 1...	203.76	3.023
P16284	Platelet endothelial cell adhesion ...	258.99	2.187

P07359	Platelet glycoprotein Ib alpha chain	225.52	2.421
P13224	Platelet glycoprotein Ib beta chain	225.10	2.065
P14770	Platelet glycoprotein IX	205.02	2.242
P40197	Platelet glycoprotein V	226.35	2.730
P16234	Platelet-derived growth factor receptor	304.60	2.256
P09619	Platelet-derived growth factor receptor	287.02	2.332
Q8IUUK5	Plexin domain-containing protein 1	268.19	2.416
Q6UX71	Plexin domain-containing protein 2	268.61	2.434
Q9UIW2	Plexin-A1	230.12	2.244
O75051	Plexin-A2	260.66	2.432
P51805	Plexin-A3	193.30	2.529
Q9HCM2	Plexin-A4	266.10	2.424
O43157	Plexin-B1	203.34	2.851
O15031	Plexin-B2	233.05	2.659
Q9ULL4	Plexin-B3	191.21	2.739
O60486	Plexin-C1	246.44	2.630
O00592	Podocalyxin	220.92	3.050
Q9NZ53	Podocalyxin-like protein 2	296.65	2.383
Q86YL7	Podoplanin	270.29	2.198
P15151	Poliovirus receptor	266.52	2.467
P01833	Polymeric immunoglobulin receptor	222.17	2.453
Q8N131	Porimin	171.54	2.764
Q6ISU1	Pre T-cell antigen receptor alpha	184.10	2.023
P35070	Probetacellulin	312.54	2.447
P01133	Pro-epidermal growth factor	271.96	2.511
O14944	Proepiregulin	197.90	2.761
Q9NZQ7	Programmed cell death 1 ligand 1	213.38	2.725
Q9BQ51	Programmed cell death 1 ligand 2	226.77	2.567
Q15116	Programmed cell death protein 1	230.96	2.337
Q99075	Proheparin-binding EGF-like growth factor	289.95	2.736
P16471	Prolactin receptor	248.95	2.824
Q86XR5	Proline-rich membrane anchor 1	287.02	2.569
Q07954	Pro-low-density lipoprotein receptor	262.34	2.783
Q02297	Pro-neuregulin-1, membrane-bound isoform	250.62	2.997
O14511	Pro-neuregulin-2, membrane-bound isoform	253.97	2.623
P56975	Pro-neuregulin-3, membrane-bound isoform	231.79	2.725
Q8WWG1	Pro-neuregulin-4, membrane-bound isoform	205.02	2.802
Q92824	Protein convertase subtilisin/kexin type 1	203.76	2.895
Q16549	Protein convertase subtilisin/kexin type 1	151.04	2.816
Q9P2B2	Prostaglandin F2 receptor negative regulator	186.19	2.761
Q6UW12	Prostate androgen-regulated mucin-like protein	230.12	2.538
Q9BXJ7	Protein amnionless	229.28	1.913
Q8J025	Protein APCDD1	132.21	3.002
Q4G0I0	Protein CCSMST1	173.22	2.884
P82279	Protein crumbs homolog 1	251.04	2.553
Q9BUF7	Protein crumbs homolog 3	271.96	2.246

P80370	Protein delta homolog 1	248.11	2.731
Q6UY11	Protein delta homolog 2	241.00	2.109
P0C7U0	Protein ELFN1	191.21	3.031
P58658	Protein eva-1 homolog C	229.70	2.769
P22794	Protein EVI2A	283.26	2.404
P34910	Protein EVI2B	266.52	2.886
Q5VUB5	Protein FAM171A1	269.45	2.332
A8MVW0	Protein FAM171A2	290.79	1.981
Q6P995	Protein FAM171B	232.63	2.480
Q17R55	Protein FAM187B	200.83	2.773
Q5JX71	Protein FAM209A	136.40	2.816
Q5JX69	Protein FAM209B	126.36	2.970
O95866	Protein G6b	193.30	2.290
Q9ULI3	Protein HEG homolog 1	229.28	2.429
A8MVS5	Protein HIDE1	230.54	2.305
P78504	Protein jagged-1	222.17	3.030
Q9Y219	Protein jagged-2	213.80	2.669
O76095	Protein JTB	200.83	2.861
Q8TBQ9	Protein kish-A	173.64	2.951
Q9NRX6	Protein kish-B	178.66	2.947
Q5SGD2	Protein phosphatase 1L	119.24	2.699
Q5TEA6	Protein sel-1 homolog 2	167.36	2.710
Q6UW14	Protein shisa-2 homolog	221.33	2.666
Q96DD7	Protein shisa-4	222.17	2.797
Q8N114	Protein shisa-5	216.31	2.666
Q6ZSJ9	Protein shisa-6 homolog	183.26	2.689
B4DS77	Protein shisa-9	223.84	2.936
Q7Z5N4	Protein sidekick-1	276.56	2.297
Q58EX2	Protein sidekick-2	322.59	2.030
Q9P2J2	Protein turtle homolog A	232.63	2.453
Q9UPX0	Protein turtle homolog B	215.89	2.721
Q9Y5I3	Protocadherin alpha-1	225.52	2.718
Q9Y5I2	Protocadherin alpha-10	225.52	2.718
Q9Y5I1	Protocadherin alpha-11	235.56	2.659
Q9UN75	Protocadherin alpha-12	225.52	2.718
Q9Y5I0	Protocadherin alpha-13	225.52	2.718
Q9Y5H9	Protocadherin alpha-2	227.19	2.761
Q9Y5H8	Protocadherin alpha-3	224.26	2.695
Q9UN74	Protocadherin alpha-4	225.52	2.718
Q9Y5H7	Protocadherin alpha-5	225.52	2.718
Q9UN73	Protocadherin alpha-6	225.52	2.718
Q9UN72	Protocadherin alpha-7	225.52	2.718
Q9Y5H6	Protocadherin alpha-8	225.52	2.718
Q9Y5H5	Protocadherin alpha-9	225.52	2.718
Q9H158	Protocadherin alpha-C1	256.48	2.442
Q9Y5I4	Protocadherin alpha-C2	246.86	2.226

Q9Y5F3	Protocadherin beta-1	287.86	1.987
Q9UN67	Protocadherin beta-10	233.47	1.987
Q9Y5F2	Protocadherin beta-11	229.28	1.987
Q9Y5F1	Protocadherin beta-12	229.28	1.987
Q9Y5F0	Protocadherin beta-13	229.28	1.987
Q9Y5E9	Protocadherin beta-14	254.39	2.280
Q9Y5E8	Protocadherin beta-15	225.10	1.966
Q9NRJ7	Protocadherin beta-16	229.28	1.987
Q9Y5E7	Protocadherin beta-2	229.28	1.987
Q9Y5E6	Protocadherin beta-3	229.28	1.987
Q9Y5E5	Protocadherin beta-4	229.28	1.987
Q9Y5E4	Protocadherin beta-5	229.28	1.987
Q9Y5E3	Protocadherin beta-6	229.28	1.987
Q9Y5E2	Protocadherin beta-7	233.47	1.987
Q9UN66	Protocadherin beta-8	204.18	1.955
Q9Y5E1	Protocadherin beta-9	233.47	1.987
Q14517	Protocadherin Fat 1	275.31	2.271
Q9NYQ8	Protocadherin Fat 2	232.63	2.721
Q8TDW7	Protocadherin Fat 3	315.89	2.021
Q6V0I7	Protocadherin Fat 4	218.40	2.856
Q9Y5H4	Protocadherin gamma-A1	263.59	2.213
Q9Y5H3	Protocadherin gamma-A10	273.63	2.202
Q9Y5H2	Protocadherin gamma-A11	284.93	2.278
O60330	Protocadherin gamma-A12	271.96	2.227
Q9Y5H1	Protocadherin gamma-A2	273.63	2.202
Q9Y5H0	Protocadherin gamma-A3	273.63	2.202
Q9Y5G9	Protocadherin gamma-A4	251.88	2.202
Q9Y5G8	Protocadherin gamma-A5	251.88	2.202
Q9Y5G7	Protocadherin gamma-A6	273.63	2.202
Q9Y5G6	Protocadherin gamma-A7	260.24	2.202
Q9Y5G5	Protocadherin gamma-A8	254.39	2.399
Q9Y5G4	Protocadherin gamma-A9	252.71	2.433
Q9Y5G3	Protocadherin gamma-B1	284.09	2.150
Q9Y5G2	Protocadherin gamma-B2	269.03	2.249
Q9Y5G1	Protocadherin gamma-B3	273.22	2.227
Q9UN71	Protocadherin gamma-B4	276.14	2.347
Q9Y5G0	Protocadherin gamma-B5	282.84	2.109
Q9Y5F9	Protocadherin gamma-B6	284.09	2.150
Q9Y5F8	Protocadherin gamma-B7	284.09	2.150
Q9UN70	Protocadherin gamma-C3	251.88	2.363
Q9Y5F7	Protocadherin gamma-C4	205.85	2.516
Q9Y5F6	Protocadherin gamma-C5	194.14	2.427
Q08174	Protocadherin-1	268.61	2.211
Q9P2E7	Protocadherin-10	262.76	2.494
Q9BZA7	Protocadherin-11 X-linked	245.60	2.322
Q9BZA8	Protocadherin-11 Y-linked	245.60	2.322

Q9NPG4	Protocadherin-12	256.06	2.666
Q96QU1	Protocadherin-15	290.79	2.407
Q96JQ0	Protocadherin-16	249.37	2.070
O14917	Protocadherin-17	226.77	2.629
Q9HCL0	Protocadherin-18	277.40	2.710
Q8TAB3	Protocadherin-19	244.35	2.635
Q8N6Y1	Protocadherin-20	164.85	3.010
O60245	Protocadherin-7	286.19	2.432
O95206	Protocadherin-8	260.24	2.625
Q9HC56	Protocadherin-9	279.91	2.447
P07949	Proto-oncogene tyrosine-protein kin...	237.23	2.594
P08922	Proto-oncogene tyrosine-protein kin...	220.08	2.642
P01135	Protransforming growth factor alpha	302.08	2.782
P16109	P-selectin	166.94	2.842
Q14242	P-selectin glycoprotein ligand 1	272.80	2.404
Q96KV6	Putative butyrophilin subfamily 2 m...	247.69	2.653
P58550	Putative FXYD domain-containing ion...	138.49	3.063
B8ZZ34	Putative protein shisa-8	165.69	2.820
A6NJW9	Putative T-cell surface glycoprotei...	228.45	2.396
Q5T292	Putative uncharacterized protein C1...	174.89	3.067
Q8N1Y9	Putative uncharacterized protein FL...	211.71	2.439
O60894	Receptor activity-modifying protein...	217.15	2.579
O60895	Receptor activity-modifying protein...	233.89	2.855
O60896	Receptor activity-modifying protein...	230.54	2.709
P04626	Receptor tyrosine-protein kinase er...	288.28	2.385
P21860	Receptor tyrosine-protein kinase er...	205.43	2.725
Q15303	Receptor tyrosine-protein kinase er...	257.73	2.611
P36888	Receptor-type tyrosine-protein kina...	227.61	2.734
P18433	Receptor-type tyrosine-protein phos...	294.97	2.598
P23467	Receptor-type tyrosine-protein phos...	231.79	2.764
P08575	Receptor-type tyrosine-protein phos...	265.27	2.500
P23468	Receptor-type tyrosine-protein phos...	299.99	2.793
P23469	Receptor-type tyrosine-protein phos...	270.29	1.698
Q12913	Receptor-type tyrosine-protein phos...	201.67	2.609
P10586	Receptor-type tyrosine-protein phos...	278.24	2.479
P23470	Receptor-type tyrosine-protein phos...	288.70	2.931
Q9HD43	Receptor-type tyrosine-protein phos...	262.76	2.156
Q15262	Receptor-type tyrosine-protein phos...	298.74	2.362
P28827	Receptor-type tyrosine-protein phos...	298.74	2.362
Q92932	Receptor-type tyrosine-protein phos...	223.01	2.718
Q16827	Receptor-type tyrosine-protein phos...	249.78	2.411
Q15256	Receptor-type tyrosine-protein phos...	261.50	2.725
Q13332	Receptor-type tyrosine-protein phos...	276.56	2.567
O14522	Receptor-type tyrosine-protein phos...	243.51	2.628
Q92729	Receptor-type tyrosine-protein phos...	253.97	2.398
P23471	Receptor-type tyrosine-protein phos...	292.46	3.008

Q8IUW5	RELT-like protein 1	204.60	2.921
O75787	Renin receptor	216.31	2.936
Q02846	Retinal guanylyl cyclase 1	197.48	2.602
P51841	Retinal guanylyl cyclase 2	209.62	3.044
Q6H3X3	Retinoic acid early transcript 1G p...	204.60	2.571
Q9ULK6	RING finger protein 150	247.69	2.499
Q9Y6N7	Roundabout homolog 1	201.25	2.852
Q9HCK4	Roundabout homolog 2	171.54	2.892
Q96MS0	Roundabout homolog 3	170.71	2.096
Q14162	Scavenger receptor class F member 1	212.97	2.532
Q96GP6	Scavenger receptor class F member 2	219.24	2.331
Q86VB7	Scavenger receptor cysteine-rich ty...	272.38	2.211
Q9NR16	Scavenger receptor cysteine-rich ty...	267.36	1.982
Q8WVN6	Secreted and transmembrane protein ...	217.57	2.599
Q13018	Secretory phospholipase A2 receptor	249.37	2.741
Q9BYH1	Seizure 6-like protein	212.55	2.669
Q6UXD5	Seizure 6-like protein 2	215.06	2.682
Q53EL9	Seizure protein 6 homolog	217.57	2.738
Q9H3S1	Semaphorin-4A	240.16	2.549
Q9NPR2	Semaphorin-4B	243.51	2.362
Q9C0C4	Semaphorin-4C	276.14	2.069
Q92854	Semaphorin-4D	216.31	2.056
O95754	Semaphorin-4F	192.46	2.344
Q9NTN9	Semaphorin-4G	207.53	2.583
Q13591	Semaphorin-5A	176.15	2.995
Q9H2E6	Semaphorin-6A	226.35	2.761
Q9H3T3	Semaphorin-6B	179.49	2.247
Q9H3T2	Semaphorin-6C	191.63	2.221
Q8NFY4	Semaphorin-6D	234.30	2.494
Q6UWB4	Serine protease 55	47.70	2.991
P37023	Serine/threonine-protein kinase rec...	245.18	2.318
Q96LC7	Sialic acid-binding Ig-like lectin ...	227.19	2.499
Q96RL6	Sialic acid-binding Ig-like lectin ...	196.23	2.559
Q96PQ1	Sialic acid-binding Ig-like lectin ...	206.27	2.669
Q08ET2	Sialic acid-binding Ig-like lectin ...	97.49	2.946
Q6ZMC9	Sialic acid-binding Ig-like lectin ...	206.27	2.013
A6NMB1	Sialic acid-binding Ig-like lectin ...	232.21	2.815
O15389	Sialic acid-binding Ig-like lectin ...	243.93	2.649
O43699	Sialic acid-binding Ig-like lectin ...	192.88	2.957
Q9Y286	Sialic acid-binding Ig-like lectin ...	220.08	2.675
Q9NYZ4	Sialic acid-binding Ig-like lectin ...	206.69	2.707
Q9Y336	Sialic acid-binding Ig-like lectin ...	212.97	2.599
Q9BZZ2	Sialoadhesin	233.47	1.868
Q04900	Sialomucin core protein 24	209.20	2.599
Q13291	Signaling lymphocytic activation mo...	225.94	2.833
Q9Y3P8	Signaling threshold-regulating tran...	189.95	2.644

O00241	Signal-regulatory protein beta-1	199.16	2.790
Q5TFQ8	Signal-regulatory protein beta-1 is...	206.69	2.764
Q5JXA9	Signal-regulatory protein beta-2	214.64	2.548
Q9P1W8	Signal-regulatory protein gamma	148.53	3.088
Q9UIB8	SLAM family member 5	251.04	2.097
Q96DU3	SLAM family member 6	273.22	2.458
Q9NQ25	SLAM family member 7	265.68	1.796
Q9P0V8	SLAM family member 8	223.84	2.477
Q96A28	SLAM family member 9	230.12	2.591
Q96PX8	SLIT and NTRK-like protein 1	224.26	2.589
Q9H156	SLIT and NTRK-like protein 2	243.93	2.437
O94933	SLIT and NTRK-like protein 3	245.60	2.252
Q8IW52	SLIT and NTRK-like protein 4	292.04	2.374
O94991	SLIT and NTRK-like protein 5	253.13	2.480
Q9H5Y7	SLIT and NTRK-like protein 6	261.08	2.721
Q9BQ49	Small integral membrane protein 7	186.19	2.792
A6NGZ8	Small integral membrane protein 9	227.61	2.911
Q07699	Sodium channel subunit beta-1	197.48	3.084
O60939	Sodium channel subunit beta-2	252.30	2.460
Q9NY72	Sodium channel subunit beta-3	202.09	2.805
Q8IWT1	Sodium channel subunit beta-4	276.56	2.265
Q99523	Sortilin	268.61	2.800
Q92673	Sortilin-related receptor	247.27	2.535
Q9HBV2	Sperm acrosome membrane-associated ...	310.87	2.074
W5XKT8	Sperm acrosome membrane-associated ...	176.15	2.589
Q9NY15	Stabilin-1	179.49	2.136
Q8WWQ8	Stabilin-2	198.32	2.404
Q13586	Stromal interaction molecule 1	145.18	3.237
Q9P246	Stromal interaction molecule 2	134.31	3.080
Q6UWL2	Sushi domain-containing protein 1	194.56	2.864
Q9UGT4	Sushi domain-containing protein 2	238.07	2.424
Q5VX71	Sushi domain-containing protein 4	208.36	2.710
O60279	Sushi domain-containing protein 5	245.18	2.720
Q92537	Sushi domain-containing protein 6	242.25	2.407
Q9UQF0	Syncytin-1	184.93	2.492
P18827	Syndecan-1	220.08	2.566
P34741	Syndecan-2	295.81	2.427
O75056	Syndecan-3	234.72	2.435
P31431	Syndecan-4	300.41	2.554
P09564	T-cell antigen CD7	218.40	2.502
P30203	T-cell differentiation antigen CD6	240.16	2.404
Q96H15	T-cell immunoglobulin and mucin dom...	233.89	2.537
Q495A1	T-cell immunoreceptor with Ig and I...	239.32	2.684
P06729	T-cell surface antigen CD2	251.88	2.964
P06126	T-cell surface glycoprotein CD1a	246.44	2.469
P29016	T-cell surface glycoprotein CD1b	233.05	2.833

P29017	T-cell surface glycoprotein CD1c	250.62	2.479
P04234	T-cell surface glycoprotein CD3 del...	205.43	2.821
P07766	T-cell surface glycoprotein CD3 eps...	207.53	3.331
P09693	T-cell surface glycoprotein CD3 gam...	201.25	2.669
P20963	T-cell surface glycoprotein CD3 zet...	194.97	2.719
P01730	T-cell surface glycoprotein CD4	236.81	2.339
P06127	T-cell surface glycoprotein CD5	302.50	2.848
P01732	T-cell surface glycoprotein CD8 alp...	302.50	2.848
P10966	T-cell surface glycoprotein CD8 bet...	240.58	2.487
P40200	T-cell surface protein tactile	204.18	3.083
B6A8C7	T-cell-interacting, activating rece...	174.89	3.067
P10747	T-cell-specific surface glycoprotei...	279.91	2.851
Q96GX1	Tectonic-2	149.79	2.617
Q6NUS6	Tectonic-3	167.36	2.798
Q9BZG2	Testicular acid phosphatase	205.43	2.244
P36897	TGF-beta receptor type-1	212.55	3.127
P37173	TGF-beta receptor type-2	182.00	2.955
Q96J42	Thioredoxin domain-containing prote...	184.10	2.895
Q9H3N1	Thioredoxin-related transmembrane p...	207.53	2.907
Q9Y320	Thioredoxin-related transmembrane p...	187.44	2.853
P07204	Thrombomodulin	254.81	2.667
P40238	Thrombopoietin receptor	219.24	2.461
Q9NS62	Thrombospondin type-1 domain-contai...	226.35	2.674
Q9UPZ6	Thrombospondin type-1 domain-contai...	210.87	2.821
Q9C0I4	Thrombospondin type-1 domain-contai...	169.03	2.992
P07202	Thyroid peroxidase	180.33	3.163
P13726	Tissue factor	314.22	2.381
Q7L0X0	TLR4 interactor with leucine rich r...	207.53	2.067
P33681	T-lymphocyte activation antigen CD8...	177.82	3.199
P42081	T-lymphocyte activation antigen CD8...	221.33	2.972
Q9HBG7	T-lymphocyte surface antigen Ly-9	215.89	2.791
Q15399	Toll-like receptor 1	223.43	2.715
Q9BXR5	Toll-like receptor 10	271.96	2.688
O60603	Toll-like receptor 2	221.75	2.798
O00206	Toll-like receptor 4	230.96	2.486
O60602	Toll-like receptor 5	205.43	2.458
Q9Y2C9	Toll-like receptor 6	207.11	2.928
Q9NYK1	Toll-like receptor 7	187.44	2.549
Q9NR97	Toll-like receptor 8	216.31	2.375
Q9NR96	Toll-like receptor 9	158.99	2.798
Q8IYR6	Tomoregulin-1	258.99	2.470
Q9UIK5	Tomoregulin-2	256.90	2.684
Q03167	Transforming growth factor beta rec...	168.20	2.882
O43493	Trans-Golgi network integral membra...	165.27	2.780
Q6UXZ0	Transmembrane and immunoglobulin do...	217.99	2.875
Q96BF3	Transmembrane and immunoglobulin do...	173.22	2.761

Q13445	Transmembrane emp24 domain-containi...	190.37	2.728
O14668	Transmembrane gamma-carboxyglutamic...	242.25	2.505
O14669	Transmembrane gamma-carboxyglutamic...	197.90	2.646
Q9BZD7	Transmembrane gamma-carboxyglutamic...	267.36	2.822
Q9BZD6	Transmembrane gamma-carboxyglutamic...	222.59	2.535
Q14956	Transmembrane glycoprotein NMB	18.41	3.427
Q8NEW7	Transmembrane inner ear expressed p...	224.68	2.707
Q4V9L6	Transmembrane protein 119	257.32	2.702
Q8N3G9	Transmembrane protein 130	186.19	2.897
A2VDJ0	Transmembrane protein 131-like	190.37	2.723
Q24JP5	Transmembrane protein 132A	253.55	2.383
Q14DG7	Transmembrane protein 132B	240.58	2.558
Q8N3T6	Transmembrane protein 132C	220.50	2.821
Q14C87	Transmembrane protein 132D	220.50	2.821
Q6IEE7	Transmembrane protein 132E	269.45	2.444
Q8IV31	Transmembrane protein 139	162.76	2.561
Q6P9G4	Transmembrane protein 154	291.21	2.105
Q8WZ59	Transmembrane protein 190	156.48	2.828
A6NLX4	Transmembrane protein 210	244.76	2.686
A2RRL7	Transmembrane protein 213	176.15	2.955
Q86YD3	Transmembrane protein 25	183.26	2.705
Q9BXS4	Transmembrane protein 59	184.93	3.101
Q6P7N7	Transmembrane protein 81	209.20	2.584
A2RUT3	Transmembrane protein 89	113.39	3.414
Q9P0T7	Transmembrane protein 9	233.05	2.800
Q6UXU6	Transmembrane protein 92	247.27	2.653
Q3KNT9	Transmembrane protein 95	222.17	2.332
Q86YW5	Trem-like transcript 1 protein Trem-	254.39	2.293
Q5T2D2	like transcript 2 protein Triggering	211.29	2.669
Q9NP99	receptor expressed on my... Triggering	190.37	2.594
Q9NZC2	receptor expressed on my...	223.01	2.377
Q13641	Trophoblast glycoprotein	244.76	2.397
P0DKB5	Trophoblast glycoprotein-like	238.07	2.438
O00220	Tumor necrosis factor receptor supe...	307.52	2.512
O14763	Tumor necrosis factor receptor supe...	254.81	2.512
Q9UBN6	Tumor necrosis factor receptor supe...	284.09	2.531
Q9Y6Q6	Tumor necrosis factor receptor supe...	254.39	2.435
Q9NP84	Tumor necrosis factor receptor supe...	176.15	2.564
Q92956	Tumor necrosis factor receptor supe...	191.63	2.841
P08138	Tumor necrosis factor receptor supe...	221.75	2.903
Q9Y5U5	Tumor necrosis factor receptor supe...	207.53	2.599
Q9NS68	Tumor necrosis factor receptor supe...	256.90	2.553
Q969Z4	Tumor necrosis factor receptor supe...	230.54	2.972
P19438	Tumor necrosis factor receptor supe...	250.62	2.548
P20333	Tumor necrosis factor receptor supe...	274.47	3.084
O75509	Tumor necrosis factor receptor supe...	273.63	2.543

Q93038	Tumor necrosis factor receptor supe...	184.93	2.739
P36941	Tumor necrosis factor receptor supe...	216.73	2.628
P43489	Tumor necrosis factor receptor supe...	225.10	2.236
P25942	Tumor necrosis factor receptor supe...	304.60	2.282
P25445	Tumor necrosis factor receptor supe...	171.96	2.461
P28908	Tumor necrosis factor receptor supe...	261.92	2.849
Q07011	Tumor necrosis factor receptor supe...	247.69	2.380
Q9UNE0	Tumor necrosis factor receptor supe...	263.59	2.380
Q8NBR0	Tumor protein p53-inducible protein...	191.63	2.345
P09758	Tumor-associated calcium signal tra...	304.60	2.278
O43914	TYRO protein tyrosine kinase-bindin...	212.97	2.739
Q12866	Tyrosine-protein kinase Mer	188.70	2.630
P35590	Tyrosine-protein kinase receptor Ti...	228.03	2.868
Q06418	Tyrosine-protein kinase receptor TY...	225.52	2.453
P30530	Tyrosine-protein kinase receptor UF...	254.81	2.402
P34925	Tyrosine-protein kinase RYK	267.36	3.108
Q01974	Tyrosine-protein kinase transmembra...	235.56	2.680
P78324	Tyrosine-protein phosphatase non-re...	250.62	2.689
Q9Y4X1	UDP-glucuronosyltransferase 2A1	208.36	2.568
Q6UWM9	UDP-glucuronosyltransferase 2A3	197.07	2.602
Q6NUS8	UDP-glucuronosyltransferase 3A1	156.48	2.916
Q3SY77	UDP-glucuronosyltransferase 3A2	161.50	2.512
Q96F05	Uncharacterized protein C11orf24	273.22	2.065
Q6NUJ2	Uncharacterized protein C11orf87	259.41	2.338
Q86TY3	Uncharacterized protein C14orf37	184.93	2.805
Q8NEA5	Uncharacterized protein C19orf18	193.30	2.895
Q5SY80	Uncharacterized protein C1orf101	251.04	2.376
Q5JRM2	Uncharacterized protein CXorf66	253.97	2.630
Q3SXP7	Uncharacterized protein KIAA1644	210.46	2.607
Q8IYS2	Uncharacterized protein KIAA2013	176.15	2.459
Q6UXG2	UPF0577 protein KIAA1324	140.58	3.163
A8MWY0	UPF0577 protein KIAA1324-like	161.92	2.761
Q5DID0	Uromodulin-like 1	269.87	2.381
B0FP48	Uroplakin-3b-like protein	290.37	2.244
O75445	Usherin	269.45	2.357
P19320	Vascular cell adhesion protein 1	203.34	2.859
P17948	Vascular endothelial growth factor ...	207.53	2.455
P35968	Vascular endothelial growth factor ...	267.36	2.630
P35916	Vascular endothelial growth factor ...	263.59	2.489
Q6EMK4	Vasorin	216.31	1.977
P98155	Very low-density lipoprotein recept...	179.91	2.863
Q96AW1	Vesicular, overexpressed in cancer,...	169.03	2.756
P54289	Voltage-dependent calcium channel s...	122.17	2.995
Q9NY47	Voltage-dependent calcium channel s...	156.06	2.375
Q8IZS8	Voltage-dependent calcium channel s...	144.77	2.602
Q7Z3S7	Voltage-dependent calcium channel s...	116.73	2.678

Q86XK7	V-set and immunoglobulin domain-con...	224.26	2.475
Q8N0Z9	V-set and immunoglobulin domain-con...	230.54	2.452
Q86VR7	V-set and immunoglobulin domain-con...	246.02	2.167
Q96IQ7	V-set and immunoglobulin domain-con...	236.81	2.477
Q9Y279	V-set and immunoglobulin domain-con...	242.25	2.911
Q5VU13	V-set and immunoglobulin domain-con...	219.24	2.756
A6NLU5	V-set and transmembrane domain-cont...	116.32	2.434
Q8IW00	V-set and transmembrane domain-cont...	263.17	2.819
A8MXK1	V-set and transmembrane domain-cont...	241.00	2.476
Q7Z7D3	V-set domain-containing T-cell acti...	136.82	2.947
Q9H7M9	V-type immunoglobulin domain-contai...	233.47	2.718
Q5VU97	VWFA and cache domain-containing pr...	187.44	2.946
Q9NP60	X-linked interleukin-1 receptor acc...	222.17	2.536
P60852	Zona pellucida sperm-binding protei...	231.38	2.261
Q05996	Zona pellucida sperm-binding protei...	172.38	2.514
P21754	Zona pellucida sperm-binding protei...	239.74	2.432
Q12836	Zona pellucida sperm-binding protei...	174.05	2.813
Q8TCW7	Zona pellucida-like domain-containi...	186.19	2.841
Q9Y493	Zonadhesin	241.00	2.218

APPENDIX C:

Type II Protein Hydrophobic Energies and Shannon Entropies

APPENDIX C: Type II Protein Hydrophobic Energies and Shannon Entropies

Uniprot ID	Protein Name	Hydrophobic Energy (kJ/mol)	Shannon Entropy (bits)
P08195	4F2 cell-surface antigen heavy chai...	223.84	2.718
Q9HDC9	Adipocyte plasma membrane-associate...	197.07	2.604
P28907	ADP-ribosyl cyclase/cyclic ADP-ribo...	261.92	2.527
P15144	Aminopeptidase N	227.19	2.955
P07306	Asialoglycoprotein receptor 1	245.18	2.108
P07307	Asialoglycoprotein receptor 2	197.90	3.010
Q9Y5Q5	Atrial natriuretic peptide-converti...	301.67	2.053
P21854	B-cell differentiation antigen CD72	230.54	2.298
Q5T4J0	Beta-1,3-galactosyl-O-glycosyl-glyc...	195.81	2.915
Q6ZNI0	Beta-1,3-galactosyl-O-glycosyl-glyc...	169.03	3.131
Q16585	Beta-sarcoglycan	294.97	2.470
Q6UWU4	Bombesin receptor-activated protein...	198.32	2.946
Q10589	Bone marrow stromal antigen 2	302.50	2.510
Q9UIR0	Butyrophilin-like protein 2	115.06	3.264
P21964	Catechol O-methyltransferase	290.37	1.417
Q9NNX6	CD209 antigen	151.46	2.503
P29965	CD40 ligand	200.83	3.288
P32970	CD70 antigen	238.91	2.475
Q5TAT6	Collagen alpha-1(XIII) chain	159.41	2.161
Q9UMD9	Collagen alpha-1(XVII) chain	233.05	1.875
Q86Y22	Collagen alpha-1(XXIII) chain	209.20	2.424
Q9BXS0	Collagen alpha-1(XXV) chain	222.17	2.529
Q5KU26	Collectin-12	228.03	2.910
Q8NC01	C-type lectin domain family 1 membe...	235.14	2.429
Q9P126	C-type lectin domain family 1 membe...	246.86	2.725
Q8IUN9	C-type lectin domain family 10 memb...	233.89	2.486
Q5QGZ9	C-type lectin domain family 12 memb...	235.14	2.620
Q2HXU8	C-type lectin domain family 12 memb...	216.31	2.606
Q6ZS10	C-type lectin domain family 17, mem...	215.89	2.606
Q6UVW9	C-type lectin domain family 2 membe...	223.43	2.944
Q92478	C-type lectin domain family 2 membe...	194.56	2.669
Q9UHP7	C-type lectin domain family 2 membe...	234.30	3.142
Q9UMR7	C-type lectin domain family 4 membe...	262.76	2.332
Q8WTT0	C-type lectin domain family 4 membe...	166.10	2.941
Q8WXI8	C-type lectin domain family 4 membe...	241.42	2.623
Q9ULY5	C-type lectin domain family 4 membe...	154.39	3.313
Q8N1N0	C-type lectin domain family 4 membe...	200.00	2.539
Q6UXB4	C-type lectin domain family 4 membe...	240.58	2.659
Q9UJ71	C-type lectin domain family 4 membe...	214.64	2.695
Q9H2X3	C-type lectin domain family 4 membe...	238.91	2.642
Q9NY25	C-type lectin domain family 5 membe...	231.79	3.046

Q6EIG7	C-type lectin domain family 6 membe...	194.97	2.987
Q9BXN2	C-type lectin domain family 7 membe...	299.57	2.358
Q6UXN8	C-type lectin domain family 9 membe...	210.46	3.214
Q8IZS7	C-type lectin-like domain family 1	176.15	3.273
Q07065	Cytoskeleton-associated protein 4	160.67	2.951
Q92629	Delta-sarcoglycan	247.27	2.790
P42658	Dipeptidyl aminopeptidase-like prot...	278.65	2.529
P27487	Dipeptidyl peptidase 4	243.51	2.347
O75923	Dysferlin	295.39	2.070
Q07108	Early activation antigen CD69	263.17	2.851
Q92838	Ectodysplasin-A	178.24	2.617
P22413	Ectonucleotide pyrophosphatase/phos...	220.08	2.797
O14638	Ectonucleotide pyrophosphatase/phos...	34.73	2.847
P42892	Endothelin-converting enzyme 1	262.76	2.256
P98073	Enteropeptidase	240.58	3.411
Q8N539	Fibrinogen C domain-containing prot...	241.00	2.256
P36269	Gamma-glutamyltransferase 5	267.36	2.189
Q6P531	Gamma-glutamyltransferase 6	165.69	2.810
Q9UJ14	Gamma-glutamyltransferase 7	190.79	2.834
P19440	Gamma-glutamyltranspeptidase 1	295.81	2.178
Q13326	Gamma-sarcoglycan	269.03	2.426
Q6ZMI3	Gliomedin	172.80	2.659
Q04609	Glutamate carboxypeptidase 2	207.53	2.690
Q07075	Glutamyl aminopeptidase	250.62	2.373
P04233	HLA class II histocompatibility ant...	134.31	3.046
Q8N608	Inactive dipeptidyl peptidase 10	267.78	2.715
Q58DX5	Inactive N-acetylated-alpha-linked ...	201.67	3.042
Q01628	Interferon-induced transmembrane pr...	262.76	2.414
P23276	Kell blood group glycoprotein	228.03	2.822
Q12918	Killer cell lectin-like receptor su...	212.13	2.643
Q9NZS2	Killer cell lectin-like receptor su...	171.96	2.553
D3W0D1	Killer cell lectin-like receptor su...	229.28	2.892
Q96E93	Killer cell lectin-like receptor su...	192.46	2.908
Q5H943	Kita-kyushu lung cancer antigen 1	134.31	3.081
Q9UIQ6	Leucyl-cystinyl aminopeptidase	273.22	2.737
P06734	Low affinity immunoglobulin epsilon...	184.10	2.720
Q06643	Lymphotoxin-beta	301.25	0.280
Q9UEW3	Macrophage receptor MARCO	222.59	2.856
P21757	Macrophage scavenger receptor types...	283.68	2.509
Q8IX19	Mast cell-expressed membrane protei...	261.50	2.856
Q9BY79	Membrane frizzled-related protein	270.29	1.963
Q16853	Membrane primary amine oxidase	308.78	2.428
P08910	Monoacylglycerol lipase ABHD2	176.56	2.665
Q9BV23	Monoacylglycerol lipase ABHD6	204.18	2.778
Q9NZM1	Myoferlin	272.38	2.486
Q9Y3Q0	N-acetylated-alpha-linked acidic di...	195.81	3.205

Q9UQQ1	N-acetylated-alpha-linked acidic di...	186.19	2.281
Q13241	Natural killer cells antigen CD94	184.10	2.527
P08473	Neprilysin	233.05	2.794
O95502	Neuronal pentraxin receptor	247.27	2.774
Q07837	Neutral and basic amino acid transp...	239.32	2.756
P26715	NKG2-A/NKG2-B type II integral memb...	299.57	2.730
P26717	NKG2-C type II integral membrane pr...	217.15	3.029
P26718	NKG2-D type II integral membrane pr...	201.25	2.737
Q07444	NKG2-E type II integral membrane pr...	217.15	3.029
O43908	NKG2-F type II integral membrane pr...	223.43	2.773
Q9HC10	Otoferlin	248.11	1.345
P78380	Oxidized low-density lipoprotein re...	214.64	2.725
P78562	Phosphate-regulating neutral endope...	221.75	2.774
O15162	Phospholipid scramblase 1	134.72	3.102
Q9NRY7	Phospholipid scramblase 2	117.57	3.293
Q9NRY6	Phospholipid scramblase 3	118.83	3.293
Q9NRQ2	Phospholipid scramblase 4	111.71	3.102
Q9BX97	Plasmalemma vesicle-associated prot...	251.46	2.648
P51164	Potassium-transporting ATPase subun...	151.46	3.273
Q12884	Prolyl endopeptidase FAP	219.24	3.106
Q6UWH4	Protein FAM198B	141.00	3.192
Q9H0X4	Protein FAM234A	259.41	2.529
A6NGU5	Putative gamma-glutamyltranspeptida...	295.81	2.178
P0C7V7	Putative signal peptidase complex c...	87.45	3.503
P46695	Radiation-inducible immediate-early...	139.33	2.940
Q6AZY7	Scavenger receptor class A member 3	261.08	2.392
Q6ZMJ2	Scavenger receptor class A member 5	267.78	2.563
P05981	Serine protease hepsin	189.54	2.720
A6NLE4	Small integral membrane protein 23	142.26	2.814
P05026	Sodium/potassium-transporting ATPas...	248.95	3.285
P14415	Sodium/potassium-transporting ATPas...	199.16	3.271
P54709	Sodium/potassium-transporting ATPas...	184.10	2.815
Q8IXA5	Sperm acrosome membrane-associated ...	176.56	0.621
Q9Y5Y6	Suppressor of tumorigenicity 14 pro...	274.47	2.280
Q9H7V2	Synapse differentiation-inducing ge...	153.13	3.195
Q9H2S6	Tenomodulin	197.48	3.066
Q9UKU6	Thyrotropin-releasing hormone-degra...	250.20	2.351
P55073	Thyroxine 5-deiodinase	182.42	3.038
P02786	Transferrin receptor protein 1	166.94	2.987
Q9UP52	Transferrin receptor protein 2	187.02	2.820
Q6ZMR5	Transmembrane protease serine 11A	253.55	2.684
Q86T26	Transmembrane protease serine 11B	220.50	2.856
O60235	Transmembrane protease serine 11D	261.50	2.725
Q9UL52	Transmembrane protease serine 11E	265.68	2.810
Q6ZWK6	Transmembrane protease serine 11F	222.59	2.761
Q9BYE2	Transmembrane protease serine 13	273.22	2.433

O15393	Transmembrane protease serine 2	186.19	2.623
P57727	Transmembrane protease serine 3	254.39	2.207
Q9NRS4	Transmembrane protease serine 4	266.94	2.242
Q9H3S3	Transmembrane protease serine 5	178.66	2.296
Q8IU80	Transmembrane protease serine 6	227.61	2.486
Q7RTY8	Transmembrane protease serine 7	242.67	2.665
Q7Z410	Transmembrane protease serine 9	212.97	2.720
Q9Y2B1	Transmembrane protein 5	141.84	3.082
P01375	Tumor necrosis factor	182.84	3.154
P50591	Tumor necrosis factor ligand superf...	195.81	3.078
O14788	Tumor necrosis factor ligand superf...	195.39	2.910
O43508	Tumor necrosis factor ligand superf...	224.68	1.991
Q9Y275	Tumor necrosis factor ligand superf...	199.58	2.642
O43557	Tumor necrosis factor ligand superf...	170.29	2.506
O95150	Tumor necrosis factor ligand superf...	187.44	2.528
Q9UNG2	Tumor necrosis factor ligand superf...	227.19	2.739
P23510	Tumor necrosis factor ligand superf...	228.86	3.180
P48023	Tumor necrosis factor ligand superf...	253.55	2.554
P32971	Tumor necrosis factor ligand superf...	225.10	2.901
P41273	Tumor necrosis factor ligand superf...	240.16	2.200
Q6NSJ0	Uncharacterized family 31 glucosida...	206.27	2.599
Q96LD1	Zeta-sarcoglycan	227.19	2.915